NASA Technical Paper 1186

A Wind-Tunnel Study of the Applicability of Far-Field Sonic-Boom Theory to the Space Shuttle Orbiter

Harry W. Carlson and Robert J. Mack

JUNE 1978

NASA

NASA Technical Paper 1186

A Wind-Tunnel Study of the Applicability of Far-Field Sonic-Boom Theory to the Space Shuttle Orbiter

Harry W. Carlson and Robert J. Mack
Langley Research Center
Hampton, Virginia

National Aeronautics
and Space Administration

**Scientific and Technical
Information Office**

1978

SUMMARY

A wind-tunnel study of the sonic-boom characteristics of a 0.0004-scale model of the space shuttle orbiter has been conducted. Pressure signatures were measured at Mach numbers of 2.8 and 4.14 and at angles of attack of 0.3^{o}, 19.0^{o}, and 41.0^{o}. To allow for observation of signature development and to provide data for extrapolation to larger distances, measurements were made at distances of from 8 to 32 body lengths. Relatively simple, purely theoretical prediction methods provided reasonably accurate estimates of bow-shock overpressure and signature impulse. Signature length predictions were less accurate, but still useful.

INTRODUCTION

A large number of wind-tunnel experimental programs (some examples are given in refs. 1 to 3) have been conducted to explore the nature of sonic-boom phenomena and to define the applicability of theoretical prediction methods. Generally, these studies demonstrated a rather remarkable ability of simple theoretical methods (based primarily on refs. 4 to 7 and described in ref. 8) to provide accurate estimates of sonic-boom characteristics for airplanes at moderate supersonic speeds. The data of reference 9 showed that the applicability of the simplified far-field theory may be extended to high supersonic Mach numbers ($M = 4.14$) and to very blunt bodies - shapes representative of entry vehicles.

The purpose of the experiments reported herein is to explore the applicability of the theory to a representative spacecraft configuration at high angles of attack and at high supersonic speeds. A 0.0004-scale model of the space shuttle orbiter (configuration 140A/B) has been tested at Mach numbers of 2.8 and 4.14 and at angles of attack up to 41.0^{o}. Pressure-signature measurements were made at distances of 8 to 32 body lengths to trace the evolution of the flow field and to provide data for extrapolation to large distances where the applicability of the theory could be assessed.

Wind-tunnel tests of a much larger scale (0.0041) model of an orbiter configuration reported in reference 10 provide signature measurements at about 1 to 1-1/2 body lengths, but those results are inappropriate for comparisons with far-field theory.

SYMBOLS

Values are given in both SI and U.S. Customary Units. The measurements and calculations were made in U.S. Customary Units.

$A(x)$ cross-sectional area normal to free-stream direction, m^2 (ft^2)

$A_e(x)$ effective cross-sectional area due to a combination of actual area and lift, $A(x) + B(x)$, m^2 (ft^2)

$B(x)$	equivalent cross-sectional area due to lift, m^2 (ft^2)
$b(x)$	local wing span, m (ft)
C_L	lift coefficient, L/qS
$C_{L,0}$	lift coefficient at zero angle of attack
$C(x)$	camber lift-distribution factor
$F(\tau)$	area distribution function
h	perpendicular distance from model centroid to measuring probe, m (ft)
h_v	altitude of aircraft (vehicle) above sea level, m (ft)
K_R	reflection factor
K_S	model or spacecraft shape factor (see eqs. (5), (6), and (7))
L	lift, N (lb)
$L(x)$	lifting force per unit longitudinal distance
l	model reference length, 1.27 cm (0.500 in.)
M	Mach number
p	reference pressure, free stream static, Pa (lb/ft^2)
Δp	incremental pressure due to model flow field, Pa (lb/ft^2)
Δp_s	incremental pressure at bow shock, Pa (lb/ft^2)
q	dynamic pressure, $\frac{\gamma}{2} pM^2$, Pa (lb/ft^2)
S	model wing reference area, 0.4 cm^2 (0.062 in^2)
Δt	pressure-signature duration from bow shock to tail shock, sec
x	distance measured in free-stream direction from body nose, m (ft)
Δx	longitudinal distance from point on pressure signature to point where signature crosses zero-pressure reference axis, m (ft)
Δx_s	longitudinal distance from bow shock to point where signature crosses zero-pressure reference axis, m (ft)
α	angle of attack, deg

β $= \sqrt{M^2 - 1}$

γ ratio of specific heats (1.4 for air)

τ dummy variable of integration measured in same direction and using same units as x

τ_o value of τ giving largest positive value of integral

A double prime is used to indicate a second derivative with respect to x.

MODEL, APPARATUS, AND TESTS

Drawings of the model and the test apparatus are presented in figure 1, and a photograph of the model is shown in figure 2. The model was constructed to a scale of 0.0004. A model of this size can, of course, represent only the gross features of the full-scale vehicle. Care was taken, however, to reproduce in scale those features which are most important in sonic-boom generation (the overall area development and the wing planform). The model reference length was taken to be 1.27 cm (0.50 in.).

A sketch of the wind-tunnel test apparatus is also shown in figure 1. The model actuator, mounted on the tunnel sidewall, provided remotely controlled longitudinal motion for the model. Pressure probes mounted on the permanent tunnel sting support system were capable of remotely controlled lateral and longitudinal movement. The tunnel sting support motion was used to place the model and the pressure sensing apparatus in the proper relative position and the model actuator was used to move the model from one position to another as the measurements were taken. The pressure-sensing apparatus was constructed such that the pressure signature of the model could be registered by the sensing probe before the bow shock impinged on the orifices of the reference probe.

The probes were very slender cones (2^o cone half-angle), each having top and bottom orifices with a diameter of 0.089 cm (0.035 in.). These probes were positioned so that a line connecting the two orifices was perpendicular to a horizontal plane containing the probe and the model. A discussion of probe selection and conditions under which simple static pressure probes can be expected to give accurate results is given in reference 9. Other considerations in providing accurate wind-tunnel measurements of sonic-boom characteristics are given in references 11 and 12.

The investigation was conducted in the Langley Unitary Plan wind tunnel at Mach numbers of 2.8 and 4.14. The test conditions provided a Reynolds number of 6.56×10^6 per meter (2.0×10^6 per foot) at both Mach numbers.

THEORETICAL CONSIDERATIONS

The character of spacecraft configurations and their operational environment permit the use of far-field theory for sonic-boom predictions. The bluntness assures a rapid coalescence of shocks to form a simple wave form early in

the propagation, and the high altitudes provide sufficient time for the formation of the classical far-field N-wave pressure signature.

The existing near-field theoretical prediction methods are inappropriate for this application. The near-field numerical prediction methods (refs. 13 and 14) have been shown to provide detailed signatures which correlate well with measured signatures for supersonic cruise airplanes. However, the so-called near-field theories are based on a supposition that the generating bodies are long and slender and the disturbances are everywhere weak. These are conditions which obviously are not met in the present investigation. It should be noted that the near-field theory gives signatures which in all cases are longer than those given by far-field theory for the same conditions;[1] whereas, as has been shown in reference 9 and as will be seen here, experimental signatures for blunt shapes and stronger disturbances are actually very much shorter than those given by far-field theory.

The far-field theory employed in this study is described in reference 6. Discussions of the theory, development of numerical methods for its implementation, and numerous correlations with experimental data are given in reference 15.

In the following equations obtained from reference 6, the characteristics of sonic-boom signatures directly under the flight path of an aircraft in level supersonic flight are related to the geometry of the aircraft and the flight conditions. The bow-shock overpressure is expressed as

$$\Delta p_s = p \frac{K_R \gamma (2\beta)^{1/4}}{\sqrt{\gamma + 1}(h)^{3/4}} \sqrt{\int_0^{\tau_o} F(\tau)\, d\tau} \tag{1}$$

The length of the positive portion of the N-wave pressure signature is given by

$$\Delta x_s = h^{1/4} \frac{\sqrt{\gamma + 1}(2)^{1/4} M^2}{\beta^{3/4}} \sqrt{\int_0^{\tau_o} F(\tau)\, d\tau} \tag{2}$$

Thus, the impulse or the area under the positive portion of the signature is

$$\int \Delta p\, dx = \frac{p}{\sqrt{h}} \frac{K_R \gamma M^2}{\sqrt{2\beta}} \int_0^{\tau_o} F(\tau)\, d\tau \tag{3}$$

The function $F(\tau)$ in equations (1), (2), and (3) depends on both the cross-sectional area and an effective cross-sectional area due to the lift distribution of the vehicle and is defined as

---

[1]Although this statement is supported by evidence from practical applications of the theories, a formal proof does not appear to be given in any of the usual references for sonic-boom theory. Such a proof could develop from the observation that for the same conditions near-field and far-field signatures have identical impulses and that near-field overpressures can be less than but not greater than overpressures on the linear-decline portion of the far-field signature.

$$F(\tau) = \frac{1}{2\pi} \int_0^{\tau} \frac{A_e''(x)}{\sqrt{\tau - x}} \, dx \tag{4}$$

where $A_e(x) = A(x) + B(x)$ with $A(x)$ representing the actual aircraft cross-sectional area and $B(x)$ the equivalent area due to lift.

For previous studies in which the bodies were slender and the disturbances propagated along lines not too different from Mach lines, area distributions as defined by supersonic area-rule concepts were employed. In this instance, where the blunt shape forces the formation of a normal shock ahead of the nose, a distribution of area normal to the free stream is believed to be more appropriate. The normal area distribution also avoids the dilemma encountered when the vehicle angle of attack exceeds the Mach angle. The problem is illustrated in the sketches at the right. As shown in the first sketch, there is little problem in interpretation of supersonic area-rule concepts when the Mach number is low and the angle of attack small. However, as shown in the second sketch, where the Mach number and the angle of attack are large there is a role reversal if the usual concepts are employed - the aircraft tail precedes the nose. Normal area distributions avoid this problem.

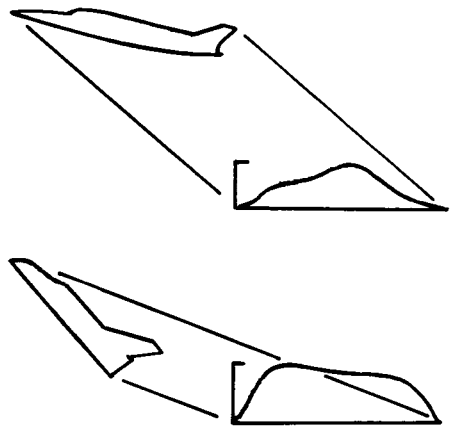

The equivalent area due to lift is defined as

$$B(x) = \frac{\beta}{2q} \int_0^x L(x) \, dx$$

There are two contributions to the lifting force $L(x)$. The first and most important contribution, that due to flat-plate wing lift, may be approximated as $(C_L - C_{L,0})qb(x)$. This assumption is exact within linearized theory for flat delta wings. For other flat wings it is a reasonable approximation. The second contribution to the lifting force results from the effects of camber at 0^o angle of attack. For the wind-tunnel configuration, camber effects are generated only by the essentially flat-bottomed fuselage. This contribution was approximated as $C_{L,0}qC(x)$ in which the assumed camber lift distribution $C(x)$ was obtained with the aid of slender-body theory. When these contributions are combined, the resultant equivalent area due to lift is

$$B(x) = \frac{\beta}{2}(C_L - C_{L,0}) \int_0^x b(x) \, dx + \frac{\beta}{2} C_{L,0} \int_0^x C(x) \, dx$$

The lift-coefficient data shown in figure 3 were obtained from reference 16. Minor adjustments were made to account for differences between the flat wing of the sonic-boom model and the twisted and cambered wing of the force model.

Effective area developments for three angles of attack and the two test Mach numbers are shown in figure 4. The areas shown include an allowance for the displacement thickness of the model boundary layer. An indication of the size of the boundary-layer contribution is given in figure 4(a). The assumed distribution of equivalent area due to camber lift (at $\alpha = 0^{o}$ the flat-plate contribution goes to zero) is also shown in figure 4(a).

After evaluation of the F-function and its integral by means of a computer program described in reference 15, signature parameters may be defined as

$$\frac{\Delta p_s}{p}\left(\frac{h}{l}\right)^{3/4} = \beta^{1/4} K_S \tag{5}$$

$$\frac{\Delta x_s}{l}\left(\frac{h}{l}\right)^{-1/4} = \frac{\gamma + 1}{\gamma}\frac{M^2}{\beta^{3/4}} K_S \tag{6}$$

$$\int \frac{\Delta p}{p}\frac{dx}{l}\left(\frac{h}{l}\right)^{1/2} = \frac{\gamma + 1}{2\gamma}\frac{M^2}{\beta^{1/2}} K_S^2 \tag{7}$$

In these equations, K_S is a shape factor determined by the computer programmed numerical solution. The shape factor is shown in figure 5 as a function of the lift parameter $(\beta/2)C_L(S/l^2)$. Numerical results for the two Mach numbers when plotted in this form agreed so closely that it was possible to use a single curve for both, and presumably for all Mach numbers in this range. Shape factors determined by the simplified sonic-boom prediction methods described in reference 17 were found to be quite similar.

By using the parameters defined in equations (5), (6), and (7), theoretical signatures for the model at a given Mach number and angle of attack may be represented by a simple N-wave. Variations with distance are taken into account in the parameters. The far-field parametric form of signature presentation is particularly useful in analysis of experimental data. It may be used, as is shown later, to assess the degree to which far-field conditions are approached and to evaluate the applicability of the theory.

RESULTS AND DISCUSSION

Measured pressure signatures are shown in figures 6 to 11. The parametric form of the signatures was chosen to help maintain uniformity in presentation of data in which peak overpressures vary from about 1 percent to 15 percent of the free-stream static pressure and in which signature length varies from about 8.5 to about 40 cm.

Superimposed on each of the measured and faired signatures is an adjusted signature. A shock front is known to be extremely thin, and measured signatures in the vicinity of a shock would be expected to display an abrupt jump in pressure were it not for the effects of model and probe vibration, probe boundary layer, and probe imperfections, as discussed in reference 9. A method, devised in reference 15, of reconstructing an idealized, inviscid steady uniform flow signature from measured data has been applied to these data. The adjustment consists of extending forward the pressure curve behind the shock and inserting a vertical line to represent an adjusted shock so that the area under the original signature is preserved.

As mentioned in the Introduction, one of the objectives of this study was to trace the evolution of the pressure signatures to the far-field condition. In figure 12, measured signatures from the three h/l stations are plotted in parametric form, which permits a study of the progressive changes in the signatures with increasing distance and of the approach to the far-field theoretical signature (eqs. (5) and (6)). For the weaker pressure signals generated at $\alpha = 0.3^{\circ}$, a stabilized far-field form appears to have been reached in about 8 model lengths. However, at the higher angles of attack, especially at $M = 4.14$, the signatures are obviously still in transition to the far-field form at the largest wind-tunnel distances.

Since the distances attainable in the wind tunnel are not sufficient in all cases for the generation of signatures which may be directly compared with the far-field theory, the extrapolation depicted in figure 13 has been employed. Adjusted measured signature parameters are plotted as a function of distance on a scale (based on a linear l/h distribution) which allows inclusion of a point at $h/l = \infty$. Fairing and extrapolation curves were graphically fitted to the data so that values of the parameters would increase or decrease monotonically and would asymptotically approach a limiting far-field value at $h/l = \infty$. Generally, the curves are well-behaved and limiting values should be defined with reasonable accuracy. The limiting values differ only slightly from the values for the largest wind-tunnel distance.

The extrapolated adjusted signature parameters are compared with theoretical predictions in figure 14. Parameters from far-field theory have again been employed. The signature parameters used in the figure have been expanded to include Mach number and γ terms. As can be seen in equations (5), (6), and (7), the parameters of figure 14 are theoretically dependent only on the shape factor K_S. In turn, as shown in figure 5, K_S for the model is represented by a single curve which is a function of the lift parameter $(\beta/2)C_L(S/l^2)$. Thus, the bow-shock overpressure, the signature length, and the signature impulse can all be represented in parameters which are theoretically a function of the lift parameter alone. Differences between the experimental data points and the theoretical curve give an indication of the ability of the theory to provide estimates of each of the signature characteristics (bow-shock overpressure, signature length, and impulse) over a wide range of operating conditions. Previous studies (refs. 1, 8, 15, and 17, for example) have demonstrated the applicability of far-field uniform-atmosphere theoretical methods to the prediction of sonic-boom phenomena in the real atmosphere, provided that proper use is made of atmospheric propagation factors.

As shown in figure 14(a), there is some tendency at the highest angle of attack for the theoretical prediction of the bow-shock overpressure to fall below the adjusted measured value. However, these discrepancies are fairly small.

The correlation of experiment and theory for signature length (fig. 14(b)) is not as good as that for overpressure. The theory should nevertheless be useful, especially for the lower angles of attack. Commonly, signature length is considered to be of lesser importance than either overpressure or impulse in defining sonic-boom acceptability.

As seen in figure 14(c), the theory provides a reasonably good prediction of signature impulse. This correlation is of particular significance because for this parameter there is no "adjusting" of experimental data.

These data in combination with that presented in reference 9 indicate that simple purely theoretical prediction methods, such as that presented in reference 17, can provide reasonably accurate estimates of spacecraft sonic-boom phenomena. Further correlations, preferably with flight-test data, are required to define more precisely whatever limitations the theory may have.

An estimated sonic-boom overpressure and signature-duration contour map for a typical atmospheric-entry flight profile of the space shuttle orbiter is shown in figure 15. This prediction was made through use of the pocket-calculator computing program described in reference 17. Very large overpressures are predicted in the immediate vicinity of the landing point. In fact, for a single point just beyond touchdown a theoretically infinite pressure is predicted. Theoretical singularities also occur all along the boundary of the footprint. The infinite pressures are of course only a mathematical concept which occurs when boom propagation ray paths become horizontal at the Earth's surface and ray areas approach zero. Little or no evidence of amplification of this nature has been found in any of the lateral-spread flight-test data (ref. 18). Under these grazing-ray conditions, atmospheric nonuniformities and turbulence tend to cause a breakup of a previously well-defined pressure signal into random noise. Accordingly, the theoretical contour lines near the boundary have been altered to indicate a monotonically decreasing overpressure. High overpressures along the flight track which result not from grazing-ray conditions but from the relative proximity of the vehicle are expected to materialize. Over a region of about 2000 km^2 (772 $miles^2$), shock overpressures of more than 100 Pa (2.09 lb/ft^2) are anticipated. It is also estimated that the shuttle produces much longer signatures than those for conventional supersonic aircraft. As indicated in figure 14(b), the theoretical predictions of signature duration may be somewhat high, perhaps by as much as 20 percent in some cases.

CONCLUDING REMARKS

An experimental and theoretical study of the sonic-boom characteristics of a 0.0004-scale model of the space shuttle orbiter has provided data for observation of signature development with distance and for extrapolation to larger distances. Purely theoretical sonic-boom prediction methods were shown to provide satisfactory estimates of signature bow-shock overpressure and

impulse at Mach numbers up to 4.14 and at angles of attack up to about 40°. This information, in combination with that for the blunt body of revolution reported in reference 9, indicates that the simplified sonic-boom prediction method described in reference 17 should provide reasonably accurate estimates of spacecraft sonic-boom characteristics for most of their operational conditions.

Langley Research Center
National Aeronautics and Space Administration
Hampton, VA 23665
April 20, 1978

REFERENCES

1. Carlson, Harry W.: Wind-Tunnel Measurements of the Sonic-Boom Characteristics of a Supersonic Bomber Model and a Correlation With Flight-Test Ground Measurements. NASA TM X-700, 1962.

2. Carlson, Harry W.; and Morris, Odell A.: Wind-Tunnel Investigation of the Sonic-Boom Characteristics of a Large Supersonic Bomber Configuration. NASA TM X-898, 1963.

3. Carlson, Harry W.; and Shrout, Barrett L.: Wind-Tunnel Investigation of the Sonic-Boom Characteristics of Three Proposed Supersonic Transport Configurations. NASA TM X-889, 1963.

4. Whitham, G. B.: The Flow Pattern of a Supersonic Projectile. Commun. Pure & Appl. Math., vol. V, no. 3, Aug. 1952, pp. 301-348.

5. Whitham, G. B.: On the Propagation of Weak Shock Waves. J. Fluid Mech., vol. 1, pt. 3, Sept. 1956, pp. 290-318.

6. Walkden, F.: The Shock Pattern of a Wing-Body Combination, Far From the Flight Path. Aeronaut. Q., vol. IX, pt. 2, May 1958, pp. 164-194.

7. Hayes, Wallace D.: Linearized Supersonic Flow. Rep. No. AL-222, North American Aviation, Inc., June 18, 1947.

8. Carlson, H. W.; and Maglieri, D. J.: Review of Sonic-Boom Generation Theory and Prediction Methods. J. Acoust. Soc. Amer., vol. 51, no. 2, pt. 3, Feb. 1972, pp. 675-685.

9. Carlson, Harry W.; and Mack, Robert J.: A Study of the Sonic-Boom Characteristics of a Blunt Body at a Mach Number of 4.14. NASA TP-1015, 1977.

10. Mendoza, Joel P.: Wind Tunnel Pressure Signatures for a 0.0041-Scale Model of the Space Shuttle Orbiter. NASA TM X-62,432, 1975.

11. Carlson, H. W.; and Morris, O. A.: Wind-Tunnel Sonic-Boom Testing Techniques. J. Aircr., vol. 4, no. 3, May-June 1967, pp. 245-249.

12. Morris, Odell A.; and Miller, David S.: Sonic-Boom Wind-Tunnel Testing Techniques at High Mach Numbers. J. Aircr., vol. 9, no. 9, Sept. 1972, pp. 664-667.

13. Middleton, Wilbur D.; and Carlson, Harry W.: A Numerical Method for Calculating Near-Field Sonic-Boom Pressure Signatures. NASA TN D-3082, 1965.

14. Hayes, Wallace D.; Haefeli, Rudolph C.; and Kulsrud, H. E.: Sonic Boom Propagation in a Stratified Atmosphere, With Computer Program. NASA CR-1299, 1969.

15. Carlson, Harry W.: Correlation of Sonic-Boom Theory With Wind-Tunnel and Flight Measurements. NASA TR R-213, 1964.

16. Chrysler Corp. Space Division: High Supersonic Stability and Control Characteristics of a 0.015-Scale (Remotely Controlled Elevon) Model 44-0 Space Shuttle Orbiter Tested in the NASA/LaRC 4-Foot UPWT (Leg 2). NASA CR-147,646, 1976.

17. Carlson, Harry W.: Simplified Sonic-Boom Prediction. NASA TP-1122, 1978.

18. Garrick, I. E.; and Maglieri, D. J.: A Summary of Results on Sonic-Boom Pressure-Signature Variations Associated With Atmospheric Conditions. NASA TN D-4588, 1968.

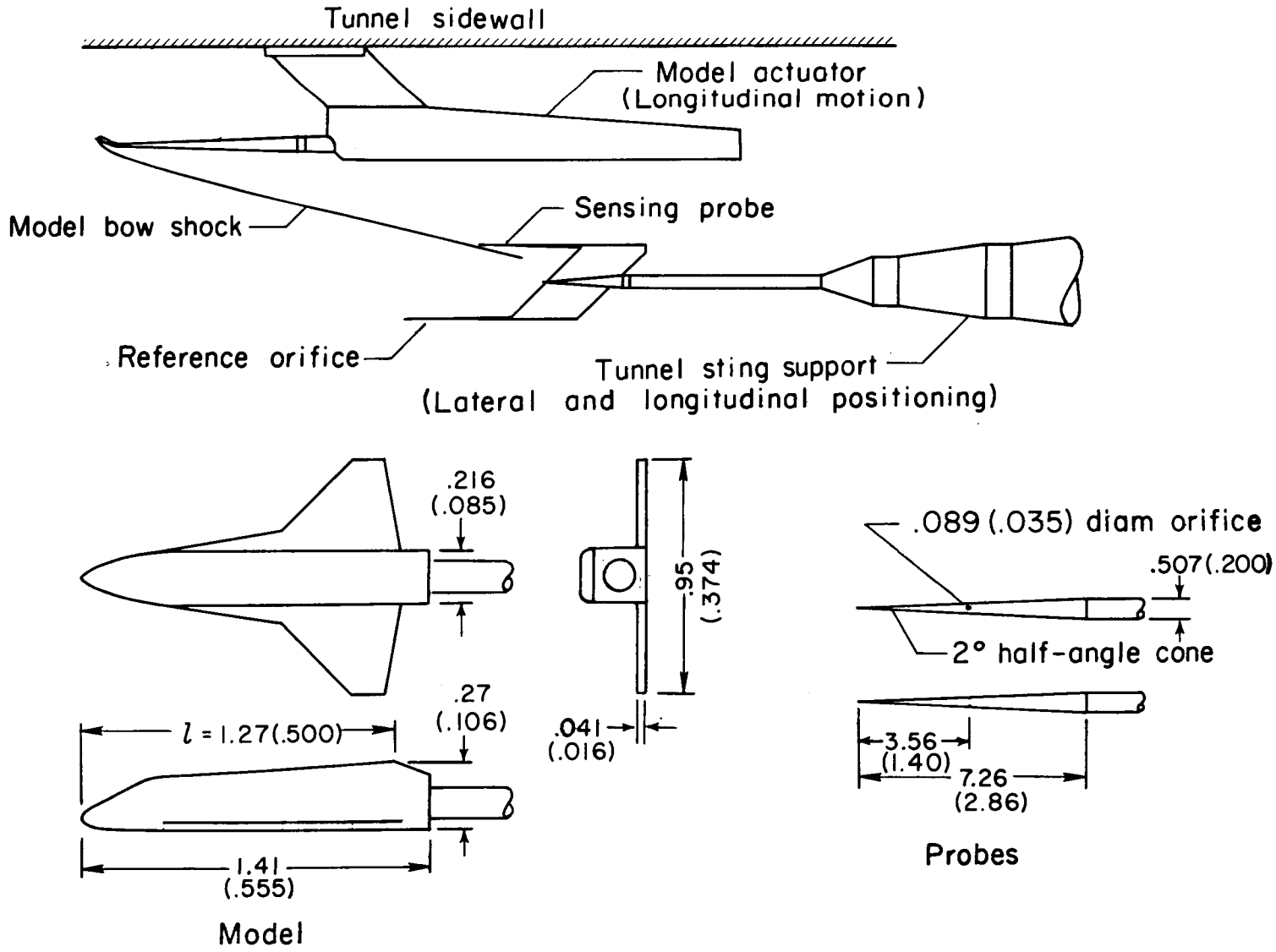

Figure 1.- Model and test apparatus. All dimensions are in cm (in.).

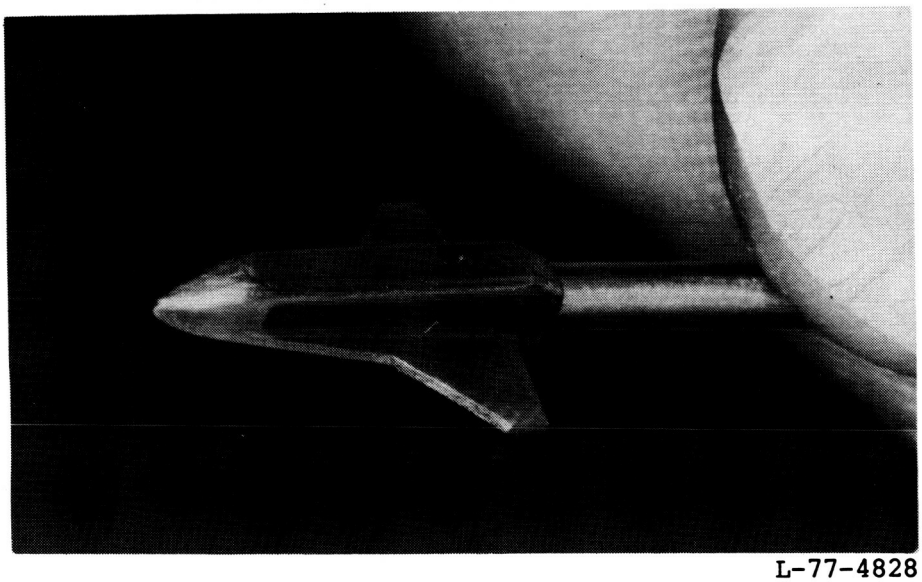

L-77-4828

Figure 2.- Photograph of model.

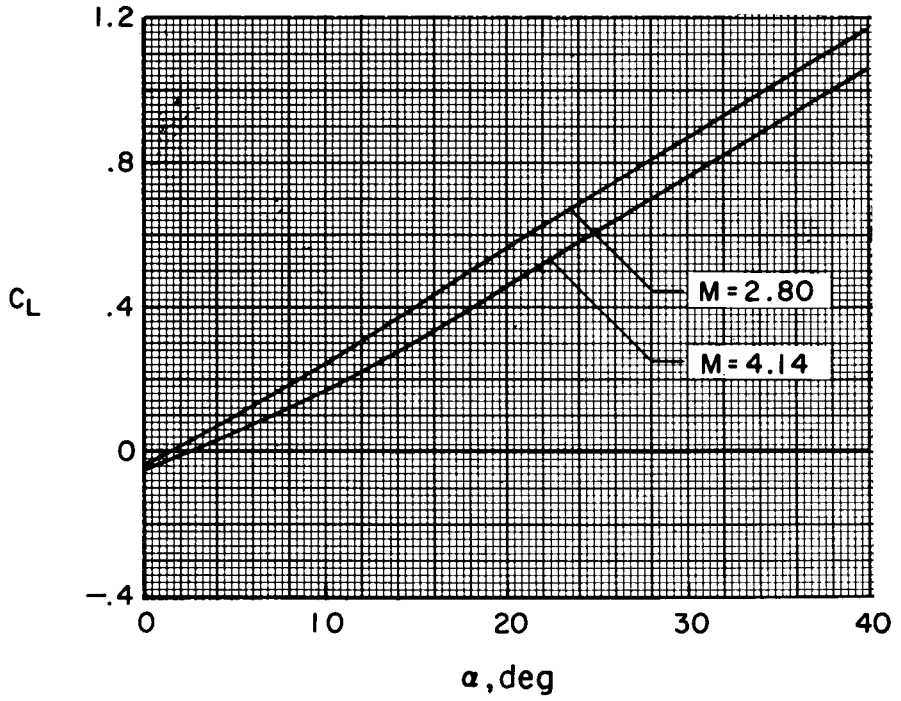

Figure 3.- Estimated lift coefficients.

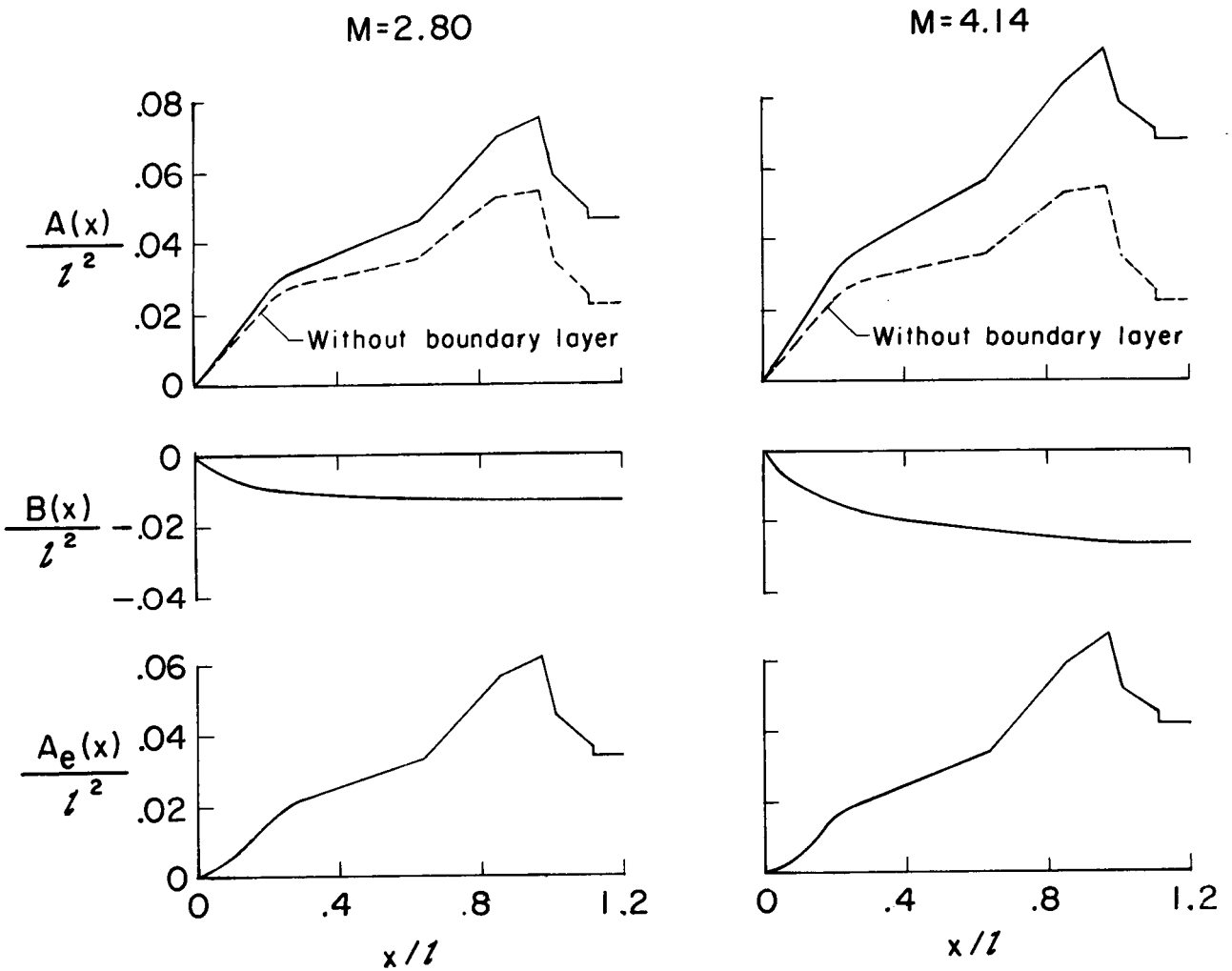

(a) $\alpha = 0^{o}$.

Figure 4.- Effective area developments.

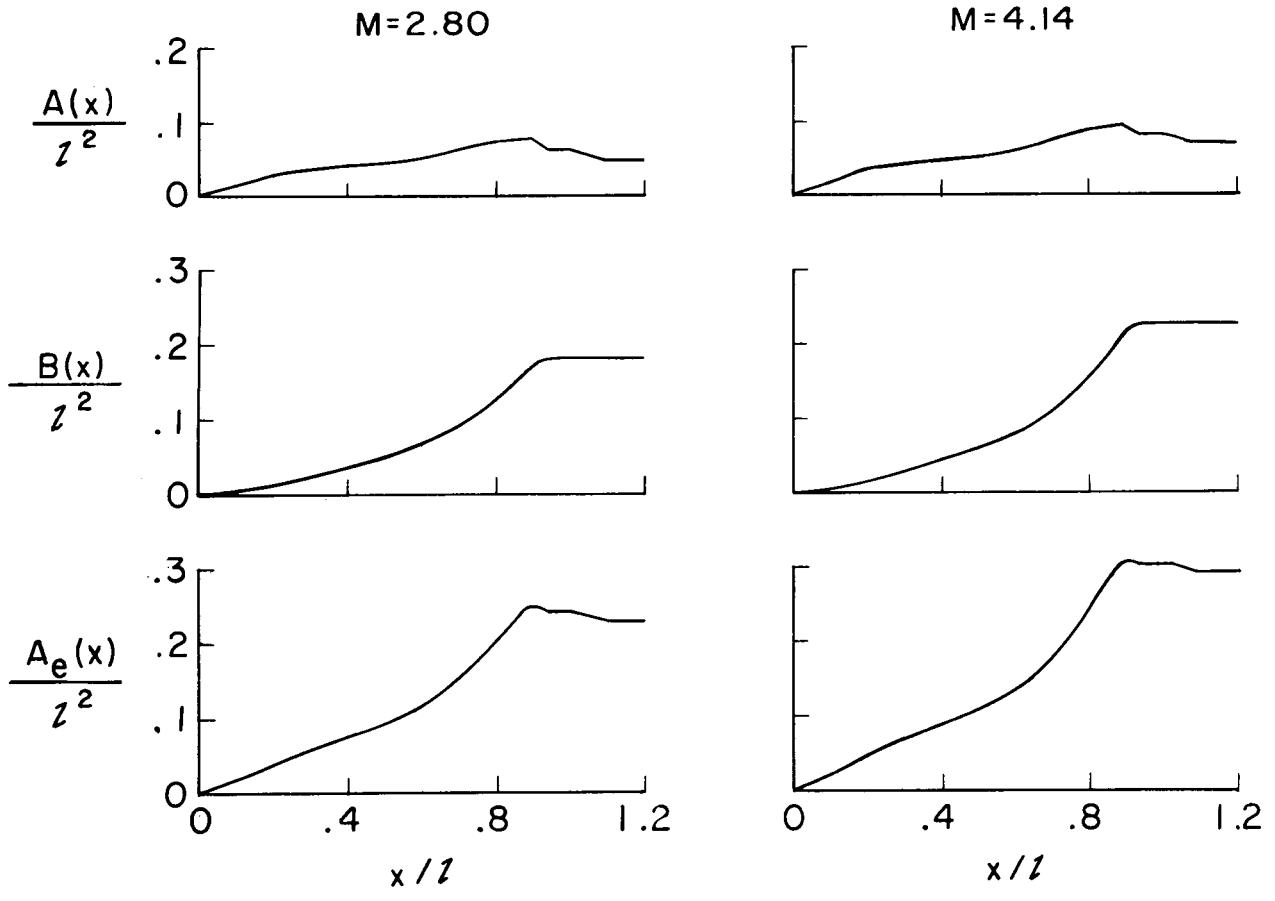

(b) $\alpha = 20^{\circ}$.

Figure 4.- Continued.

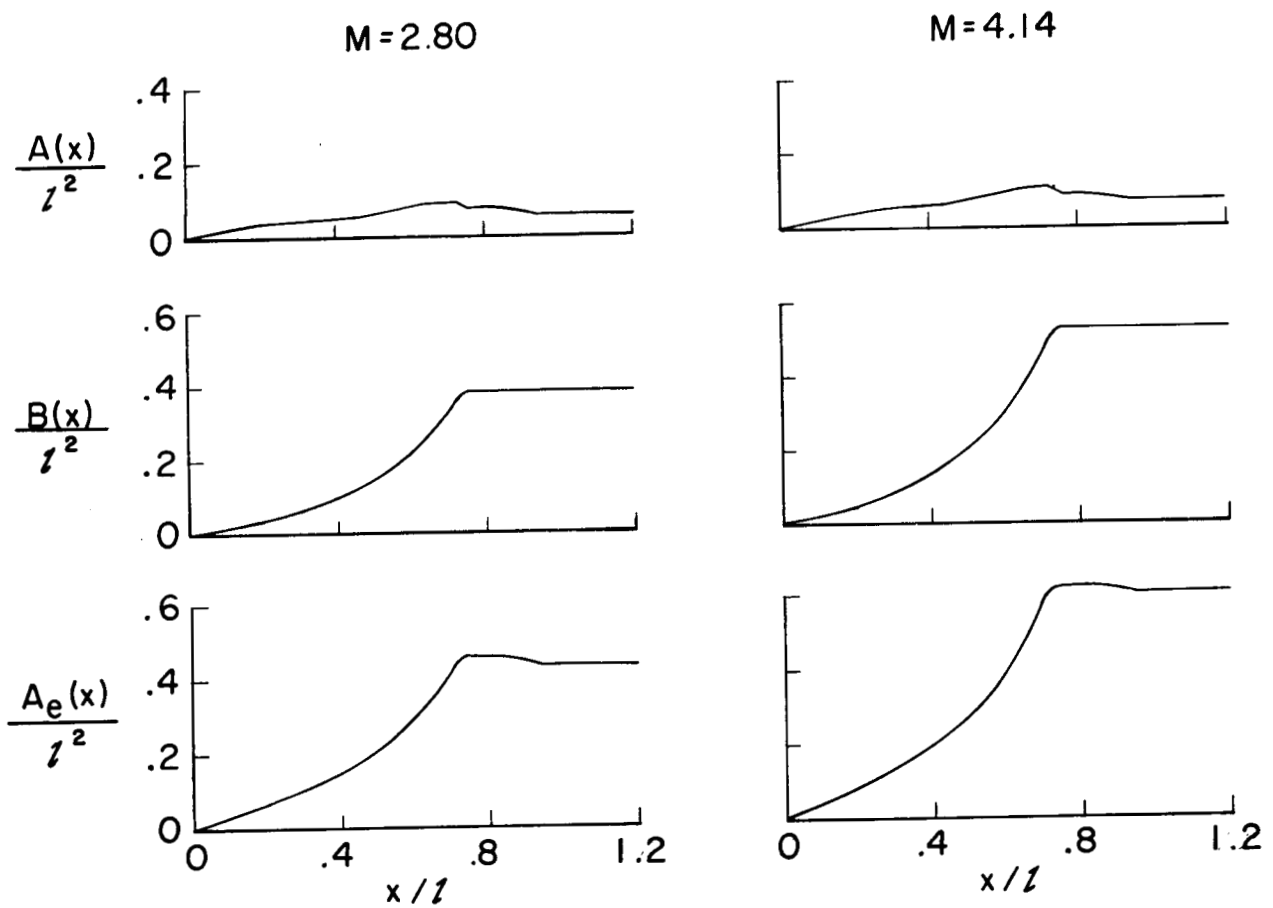

(c) $\alpha = 40^{\circ}$.

Figure 4.- Concluded.

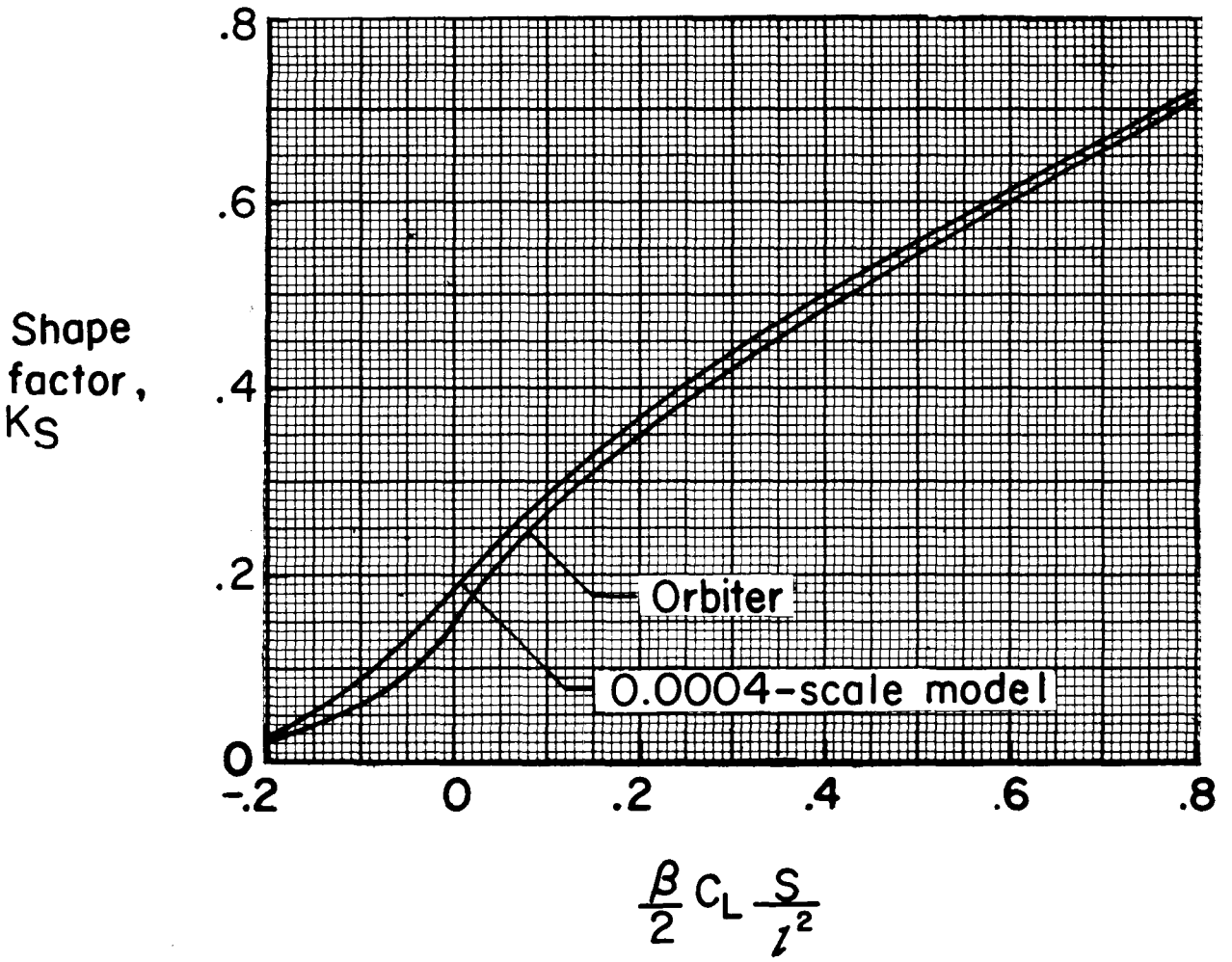

Figure 5.- Theoretical sonic-boom shape factor.

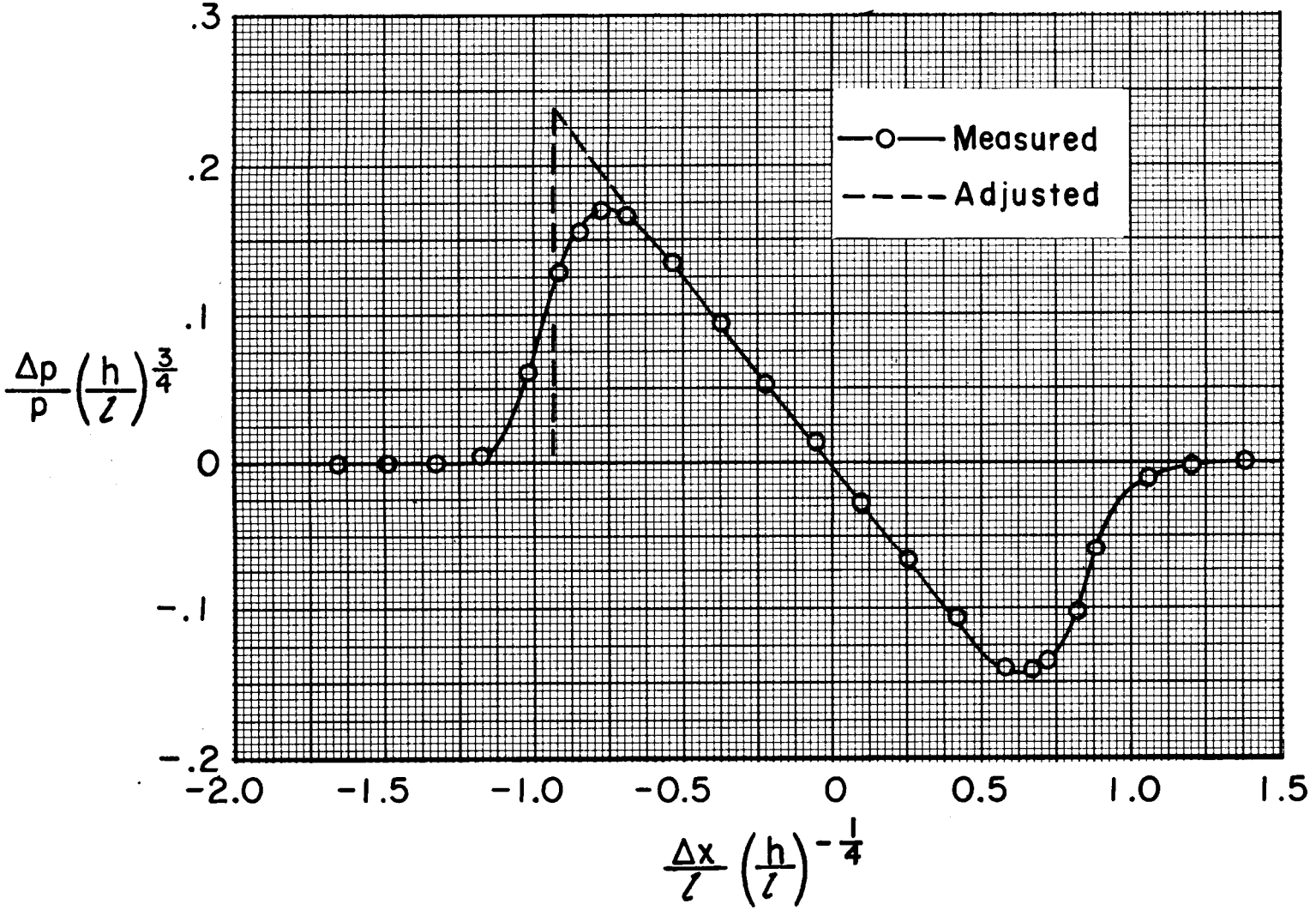

(a) $h/\ell = 8.$

Figure 6.- Measured pressure signatures. $M = 2.8$, $\alpha = 0.3^{o}$.

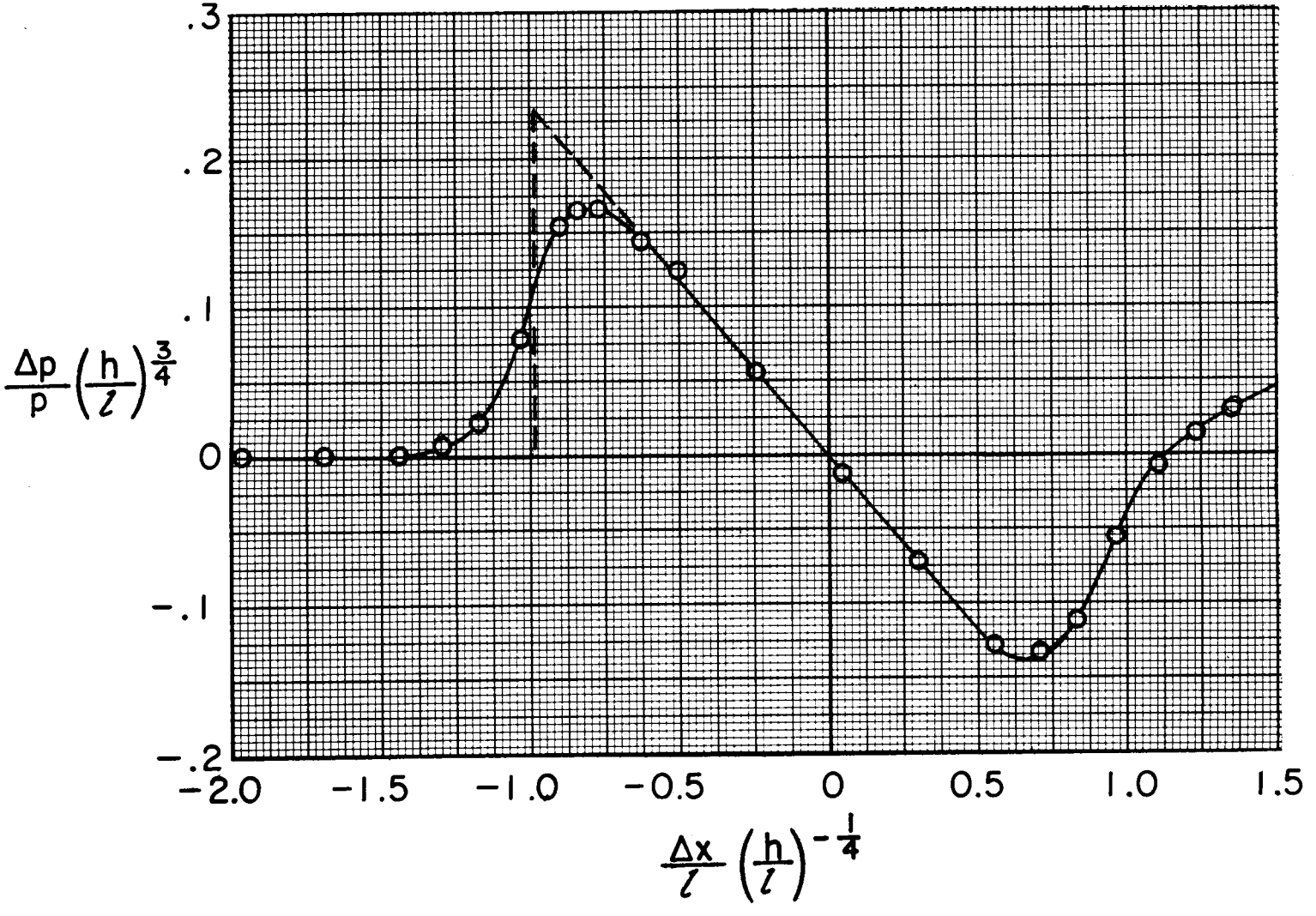

(b) $h/l = 16.$

Figure 6.- Continued.

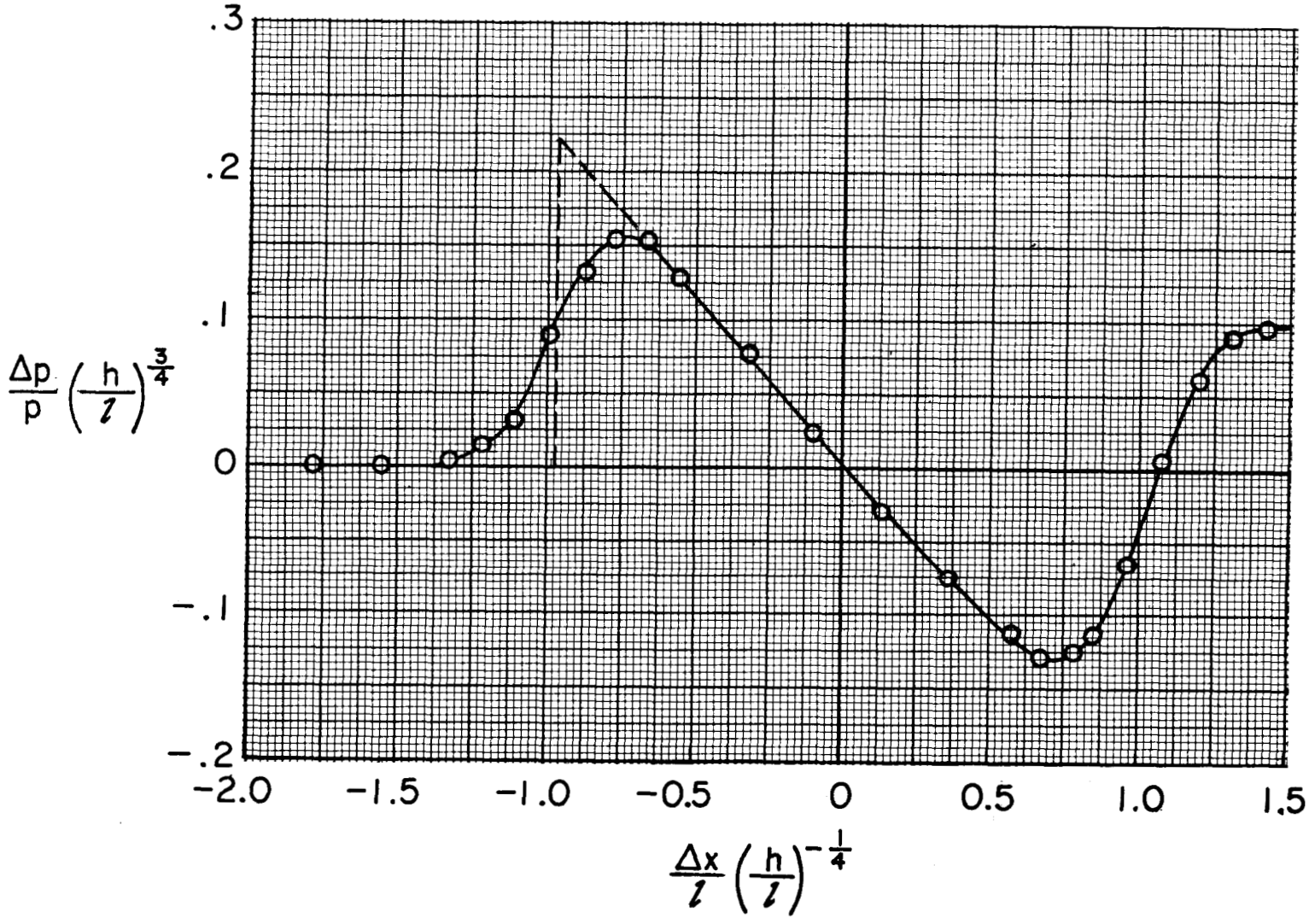

(c) $h/l = 32.$

Figure 6.- Concluded.

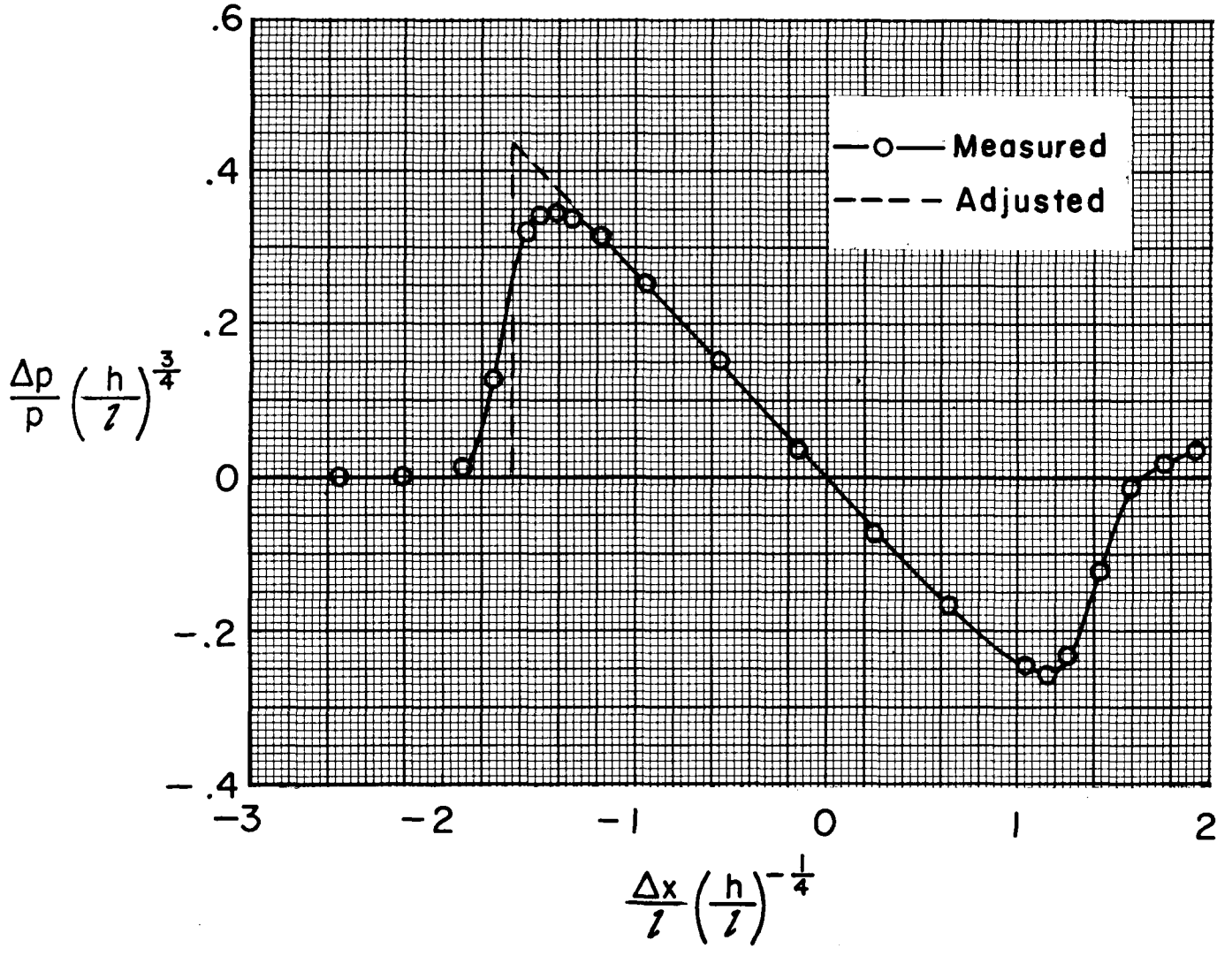

(a) $h/l = 8.$

Figure 7.- Measured pressure signatures. $M = 2.8$, $\alpha = 19.0^{\circ}$.

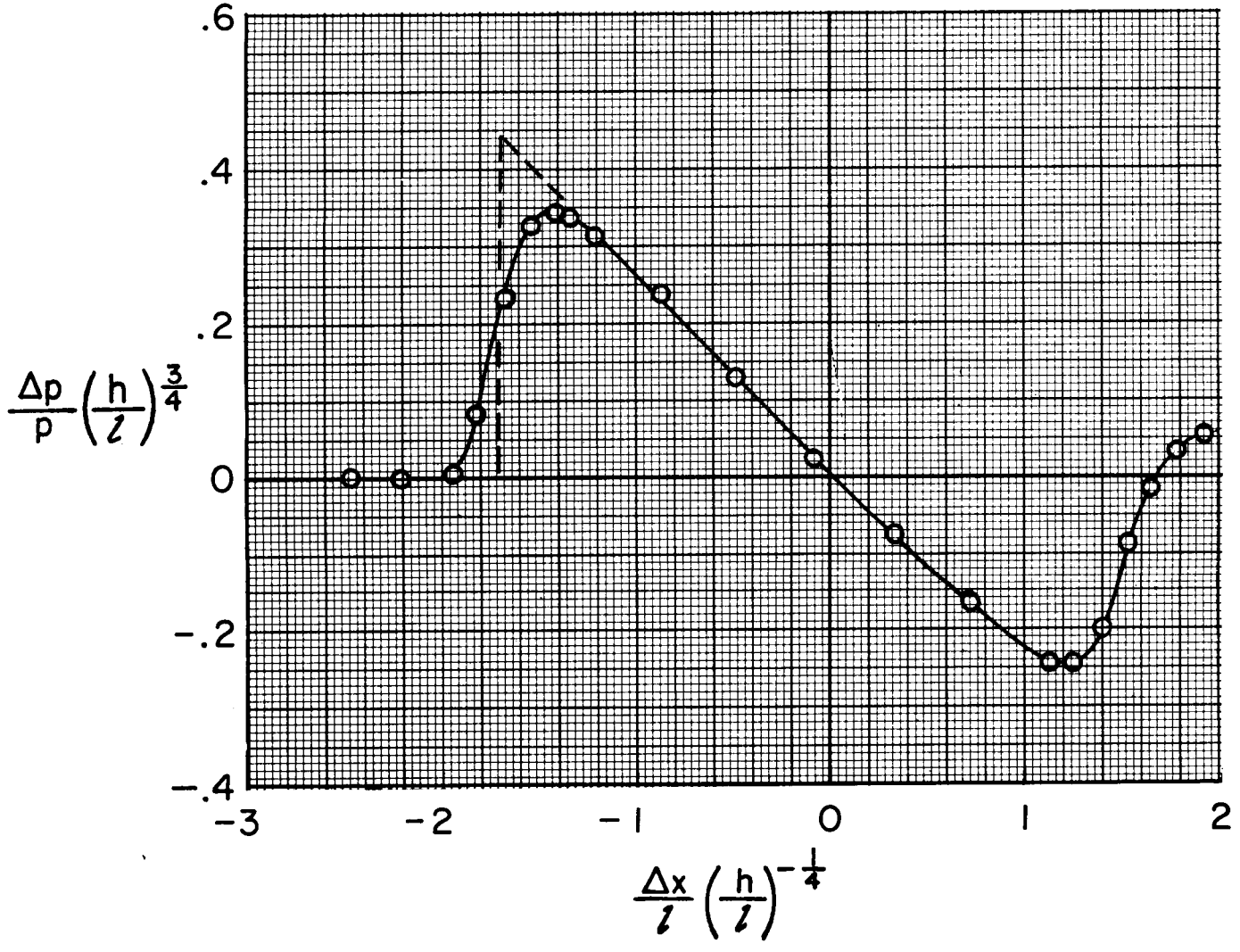

(b) $h/l = 16.$

Figure 7.- Continued.

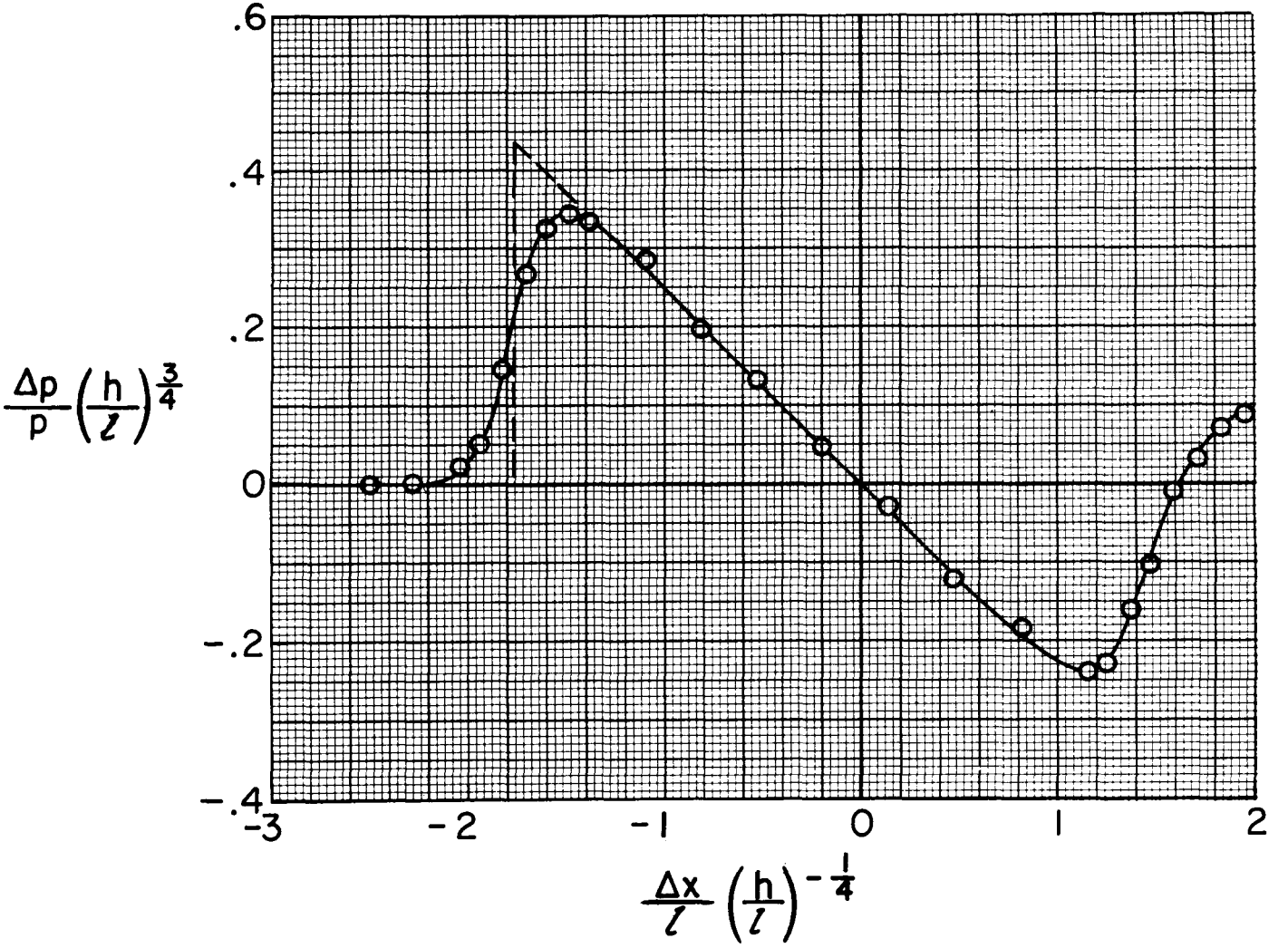

(c) $h/l = 32.$

Figure 7.- Concluded.

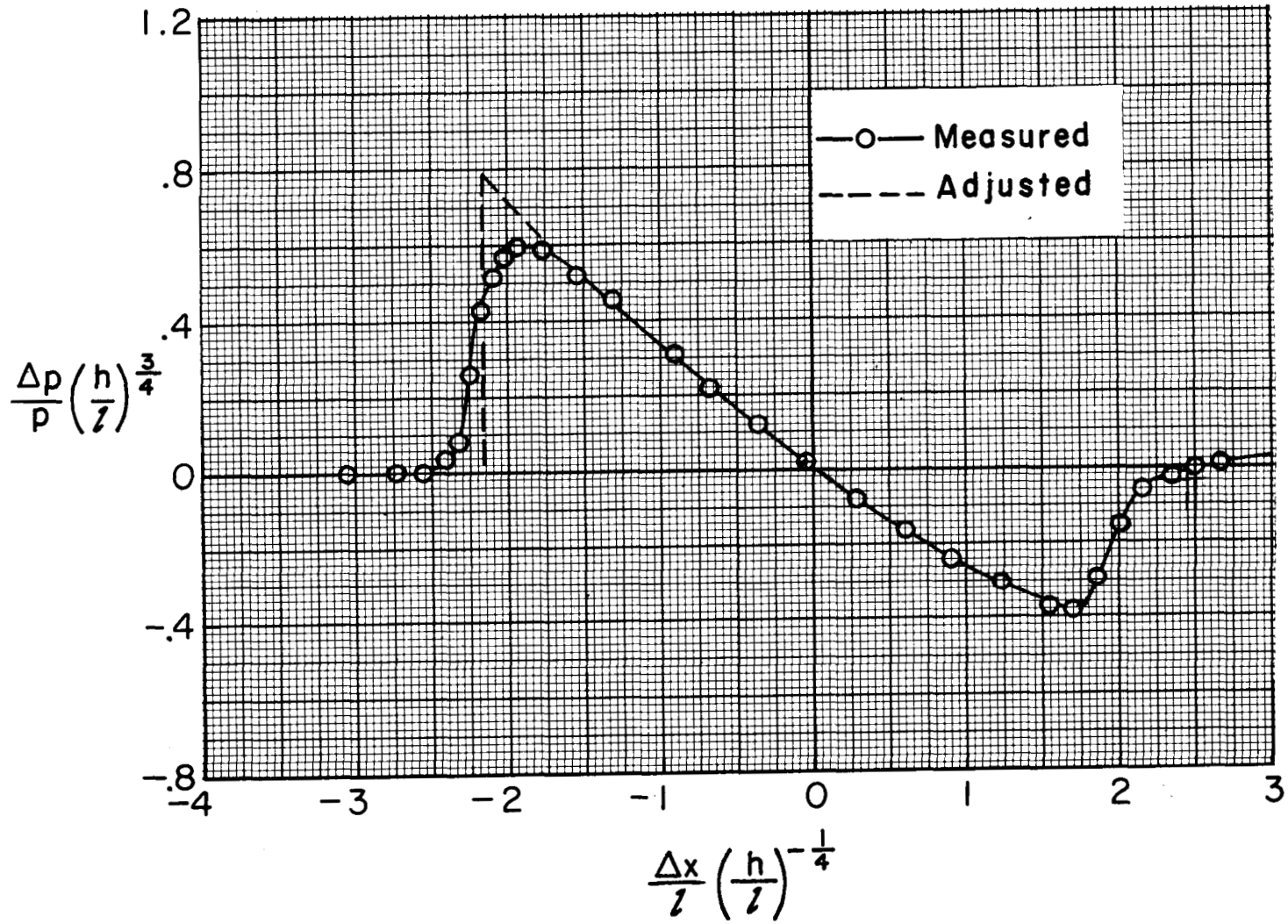

(a) $h/l = 8.$

Figure 8.- Measured pressure signatures. $M = 2.8$, $\alpha = 41.0^{o}$.

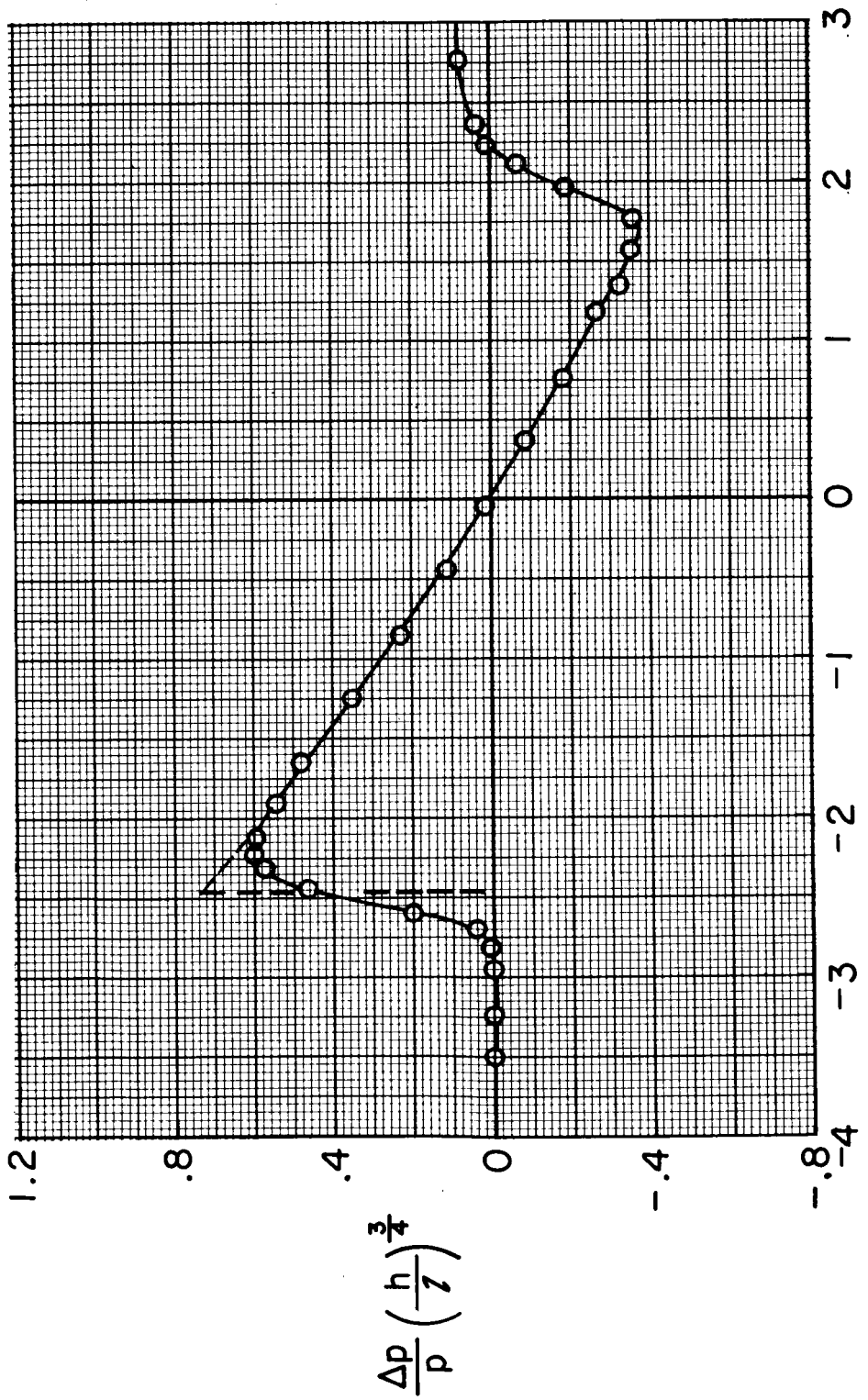

(b) $h/l = 16$.

Figure 8.- Continued.

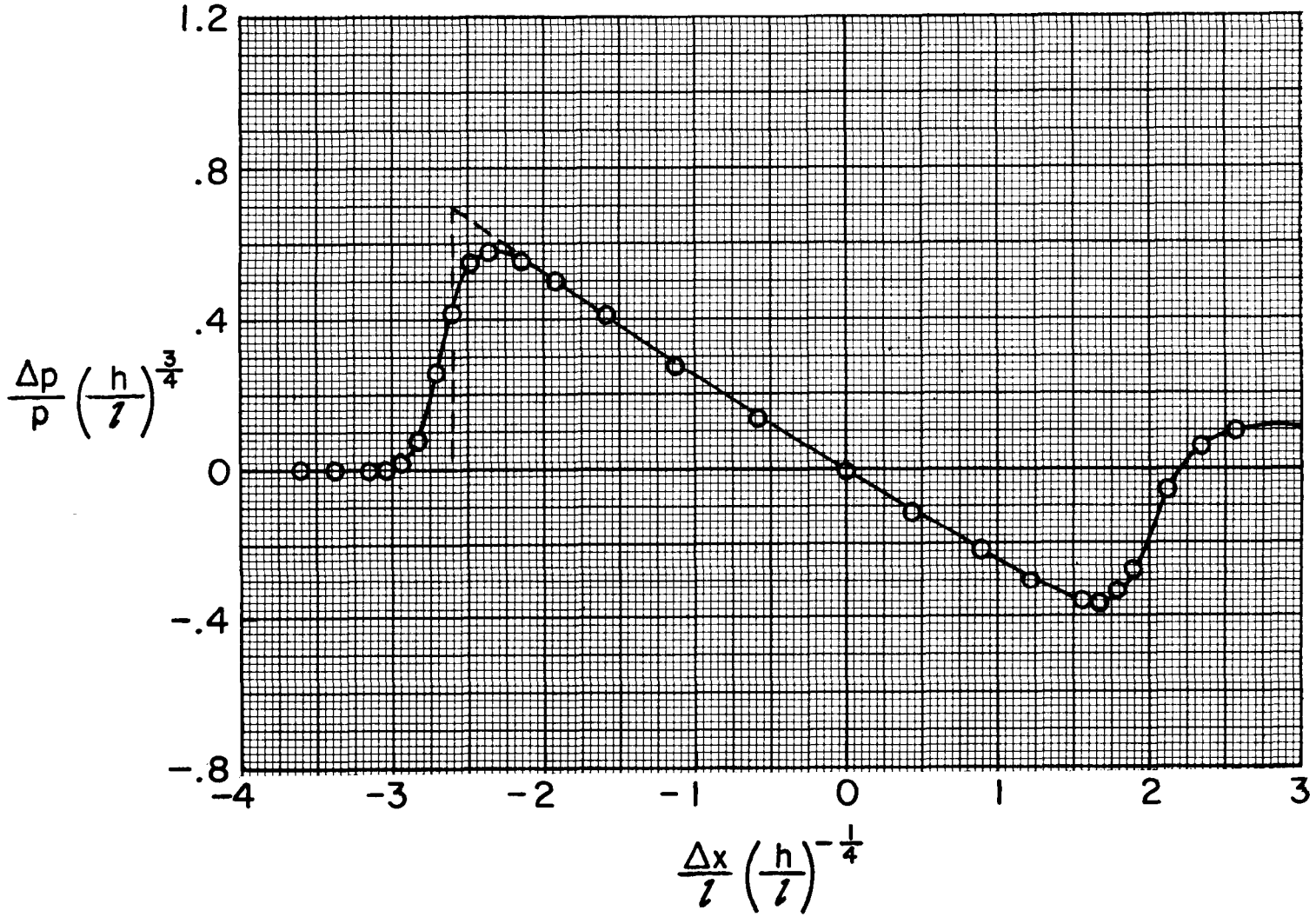

(c) $h/l = 32.$

Figure 8.- Concluded.

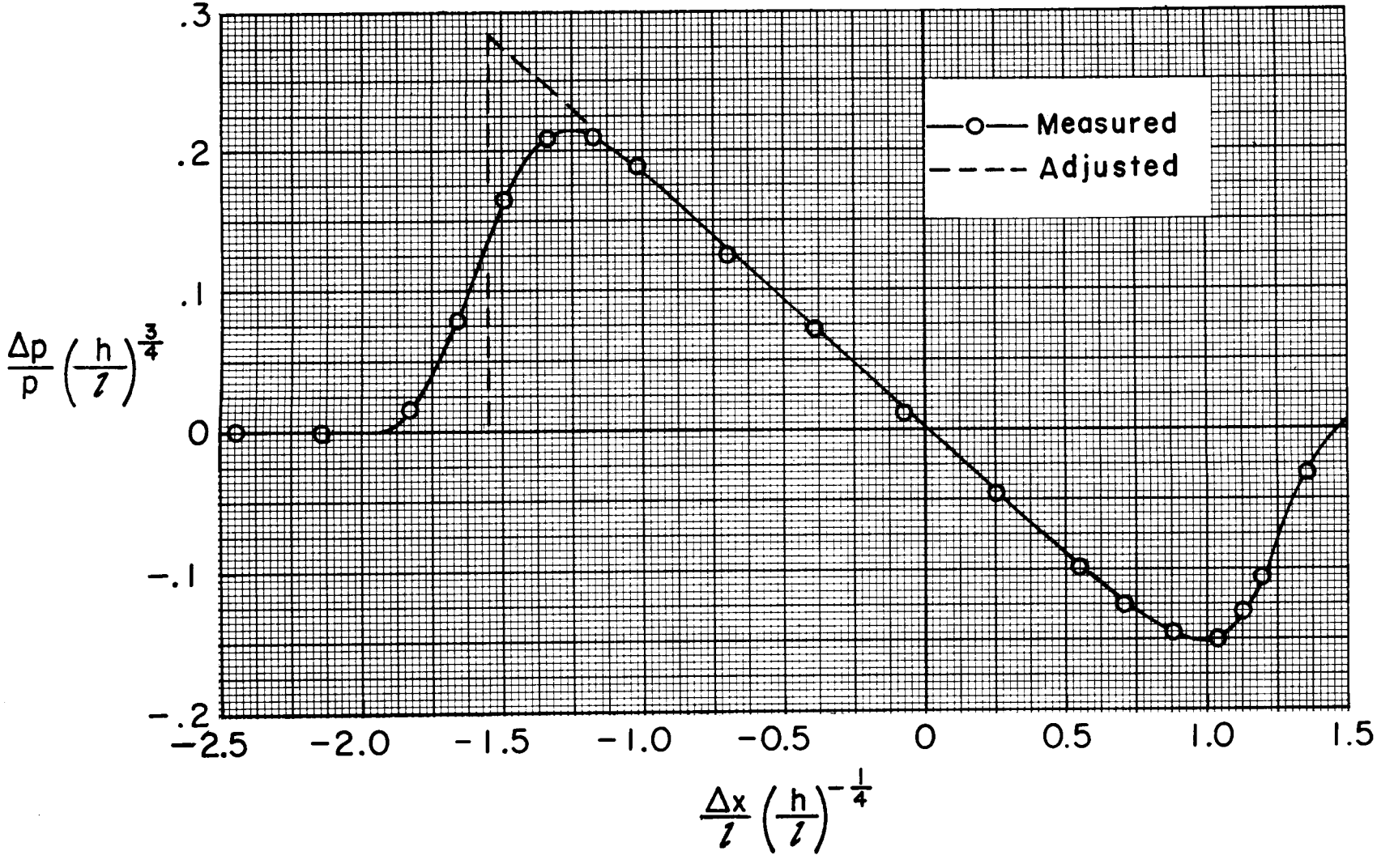

(a) $h/l = 8.$

Figure 9.- Measured pressure signatures. $M = 4.14$, $\alpha = 0.3^{o}$.

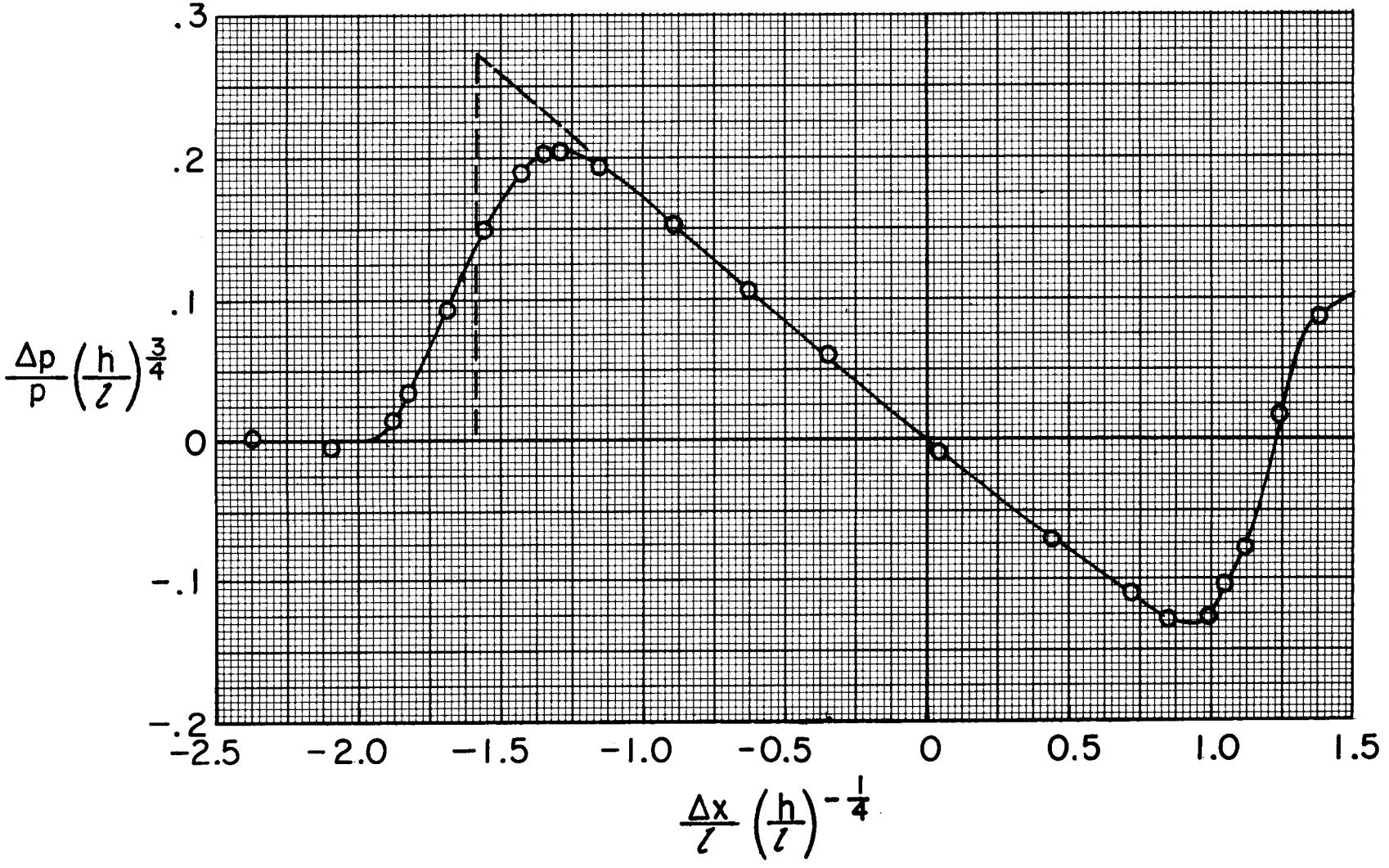

(b) $h/l = 16.$

Figure 9.- Continued.

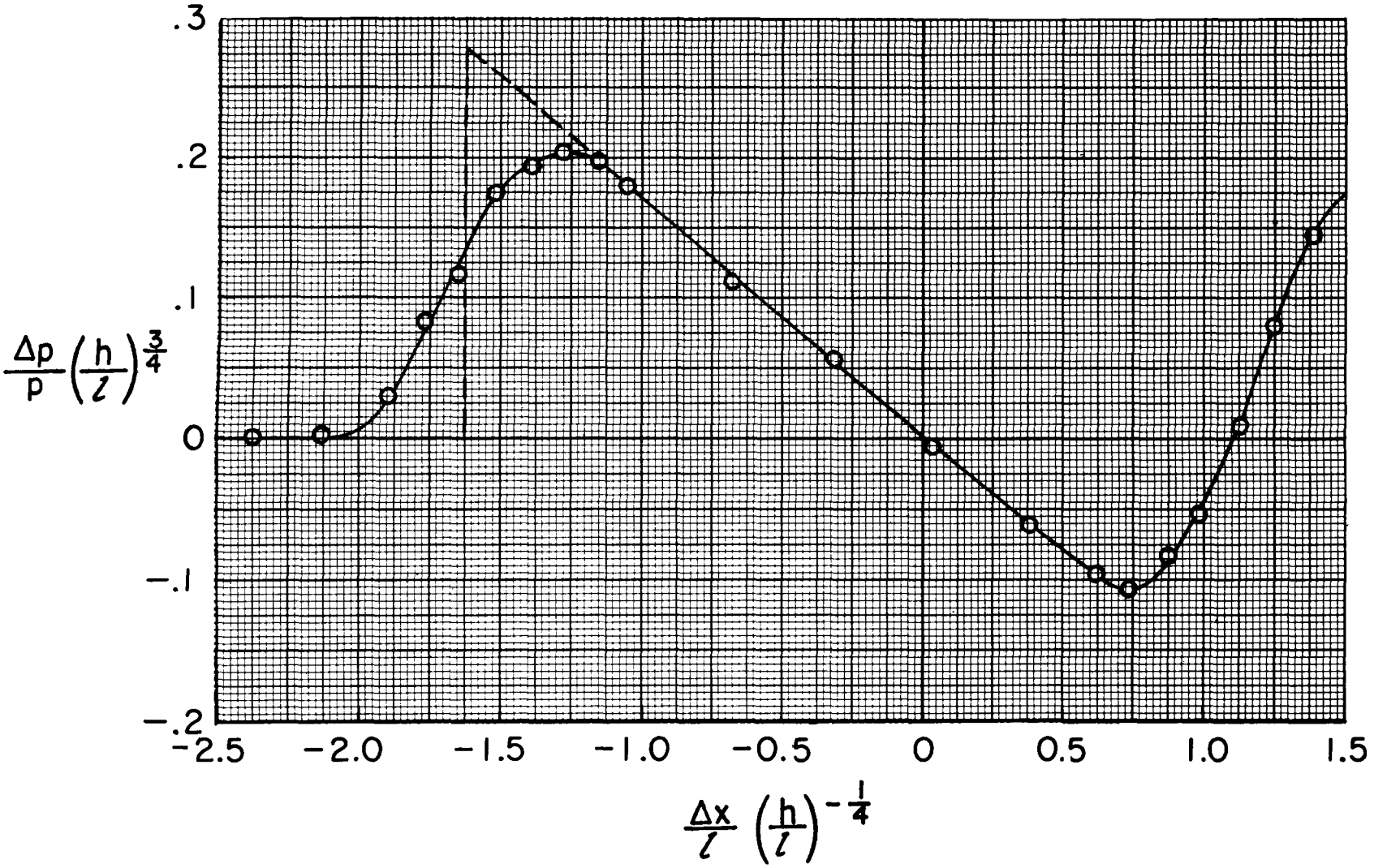

(c) $h/l = 24.$

Figure 9.- Concluded.

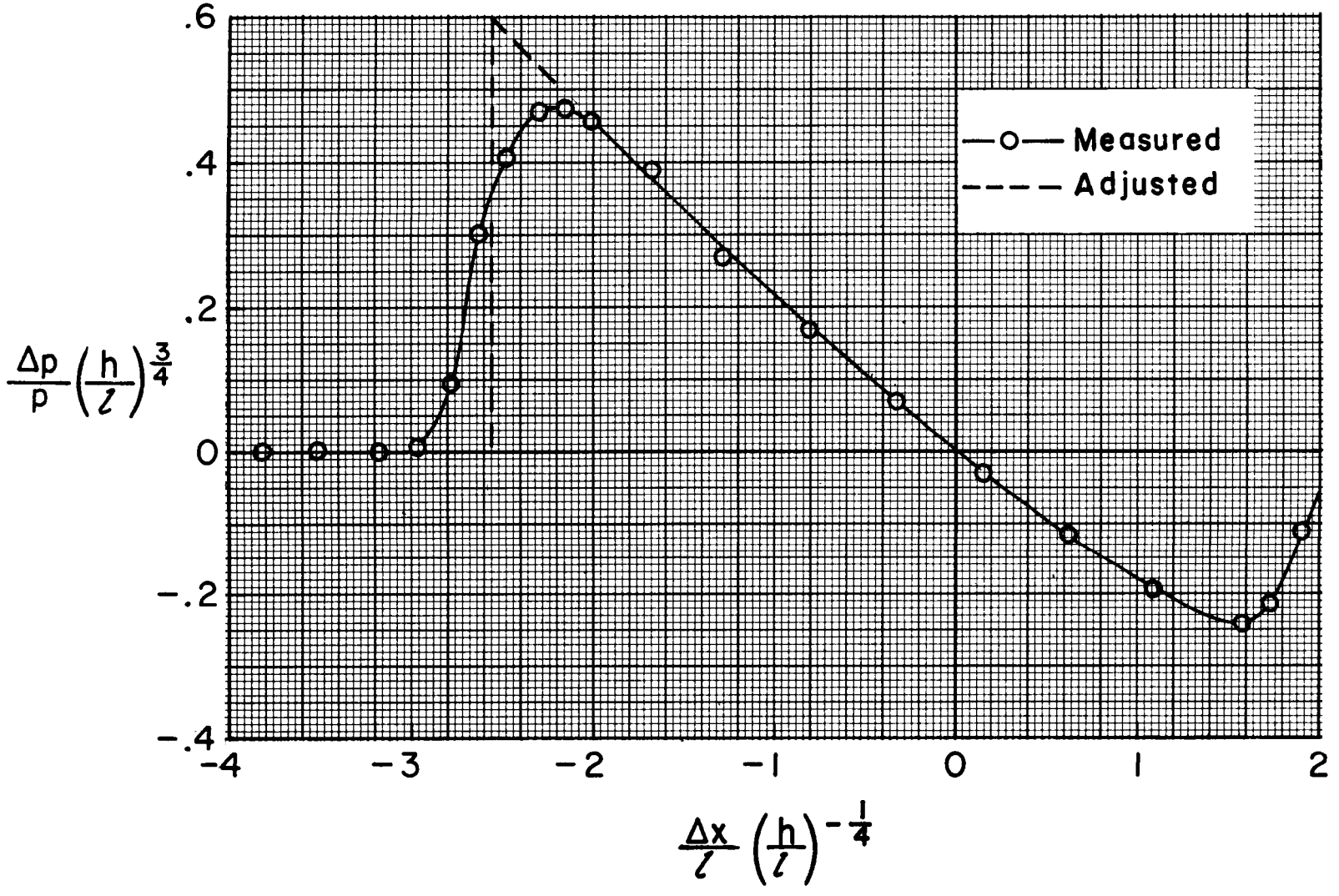

(a) $h/l = 8.$

Figure 10.- Measured pressure signatures. $M = 4.14$, $\alpha = 19.0^{\circ}$.

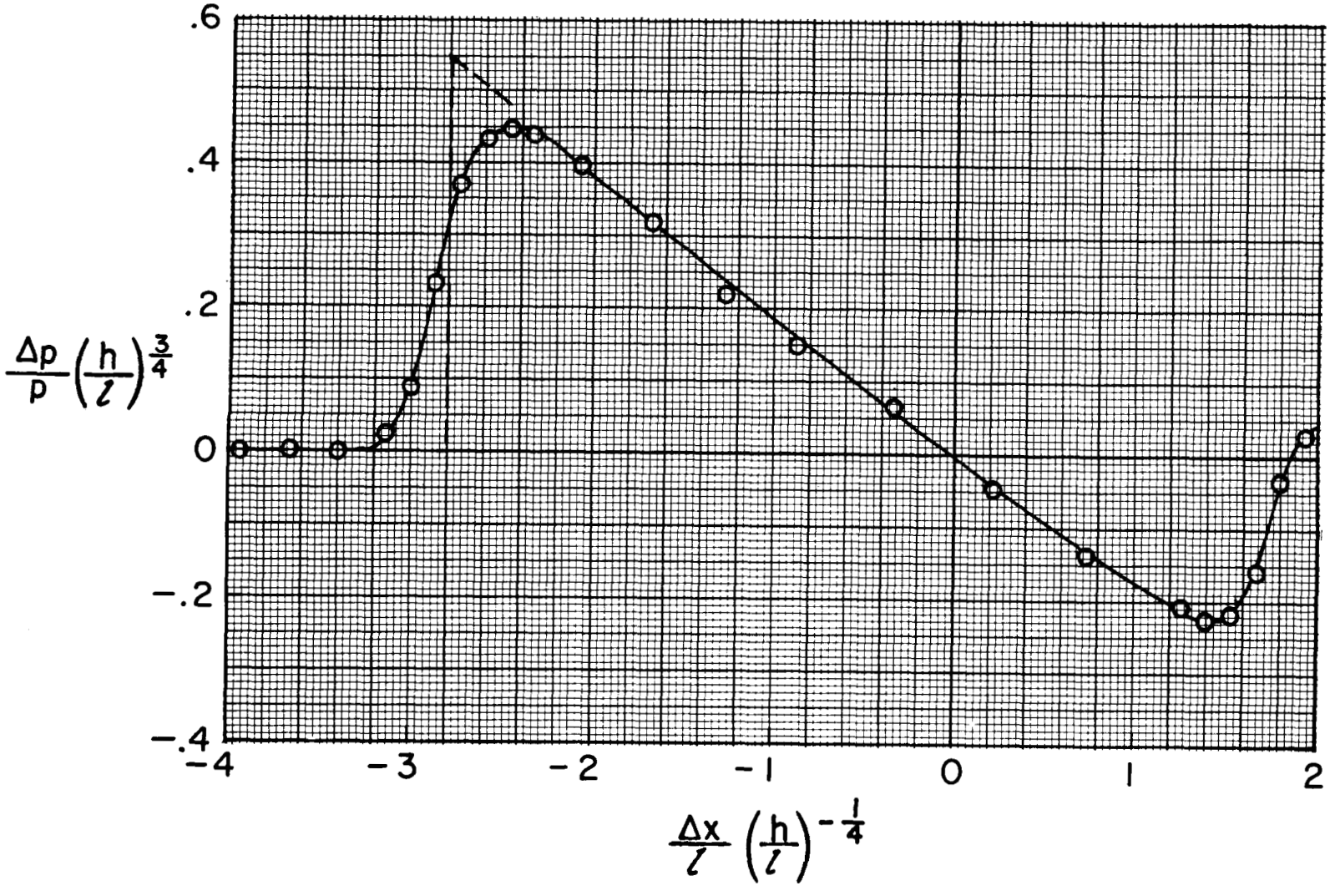

(b) $h/l = 16.$

Figure 10.- Continued.

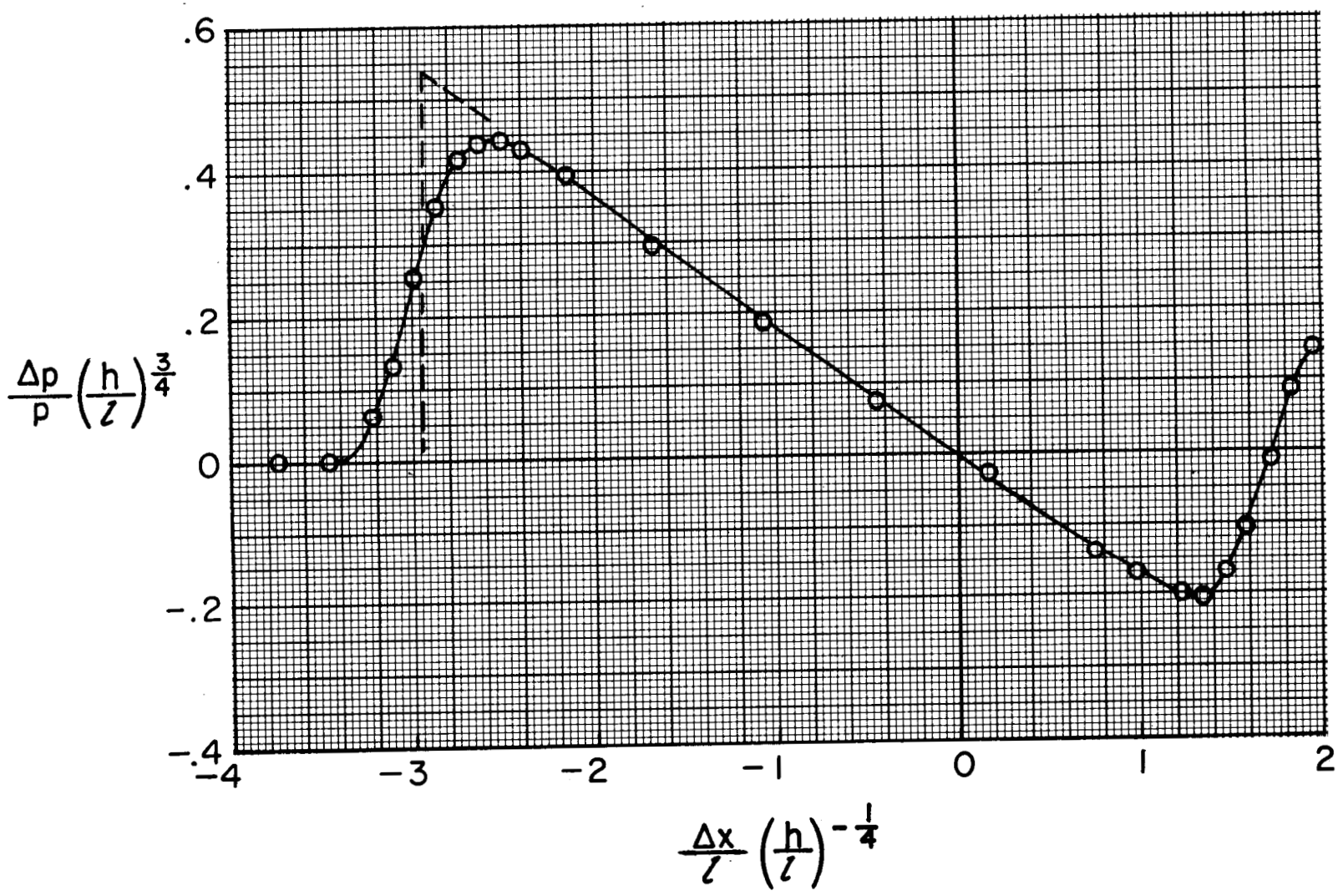

(c) $h/l = 24$.

Figure 10.- Concluded.

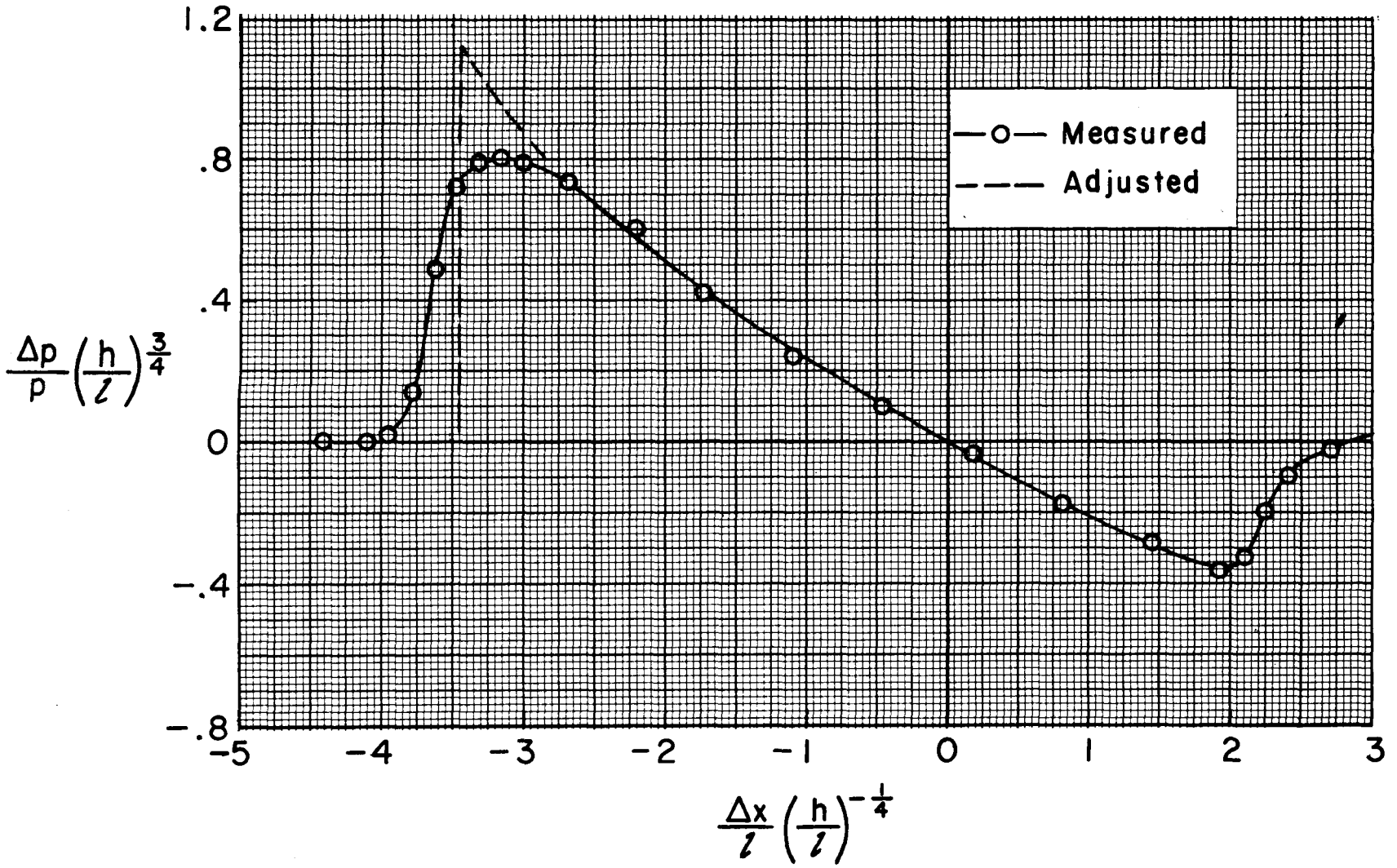

(a) $h/l = 8.$

Figure 11.- Measured pressure signatures. $M = 4.14$, $\alpha = 41.0^{\circ}$.

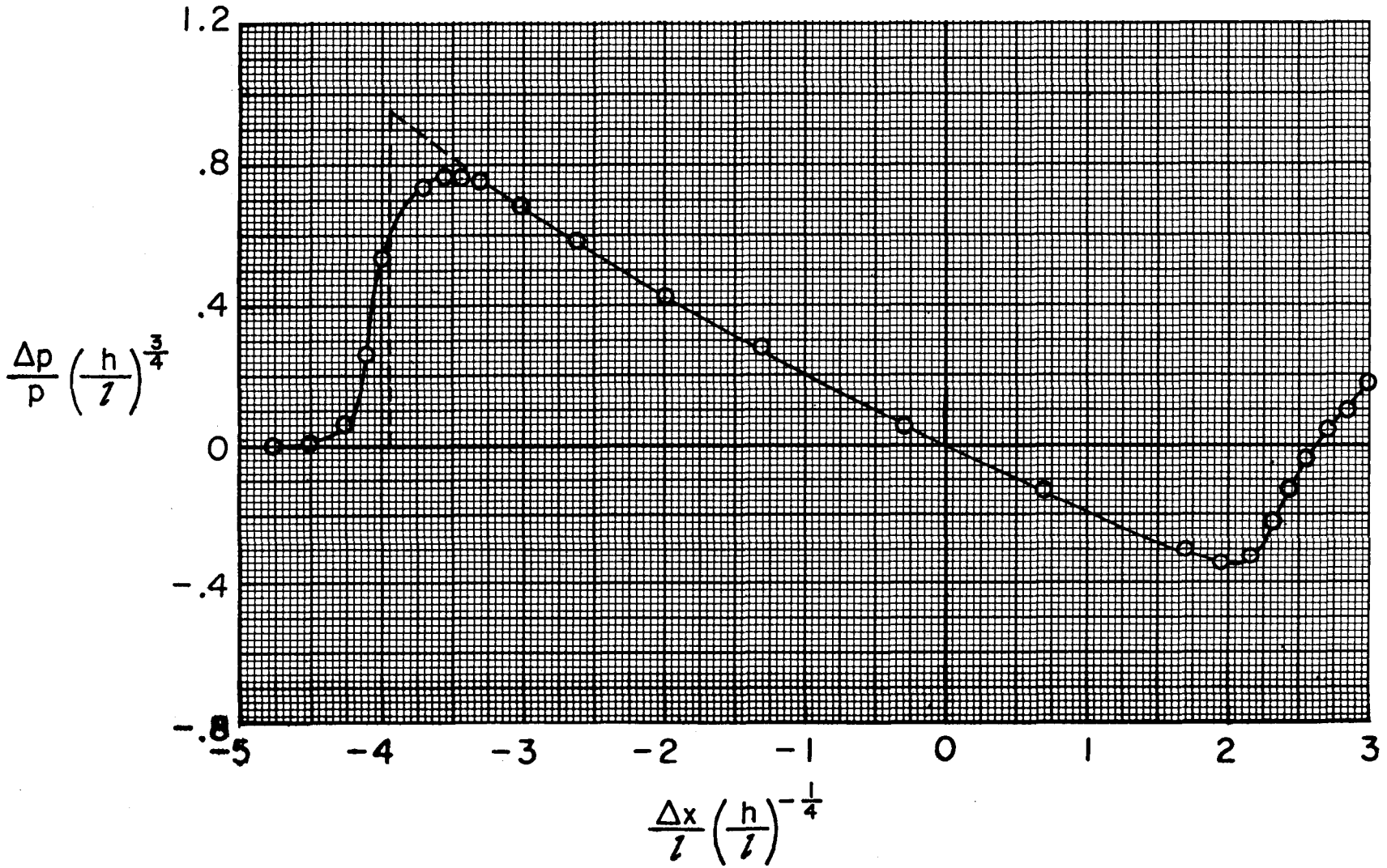

(b) $h/l = 16$.

Figure 11.- Continued.

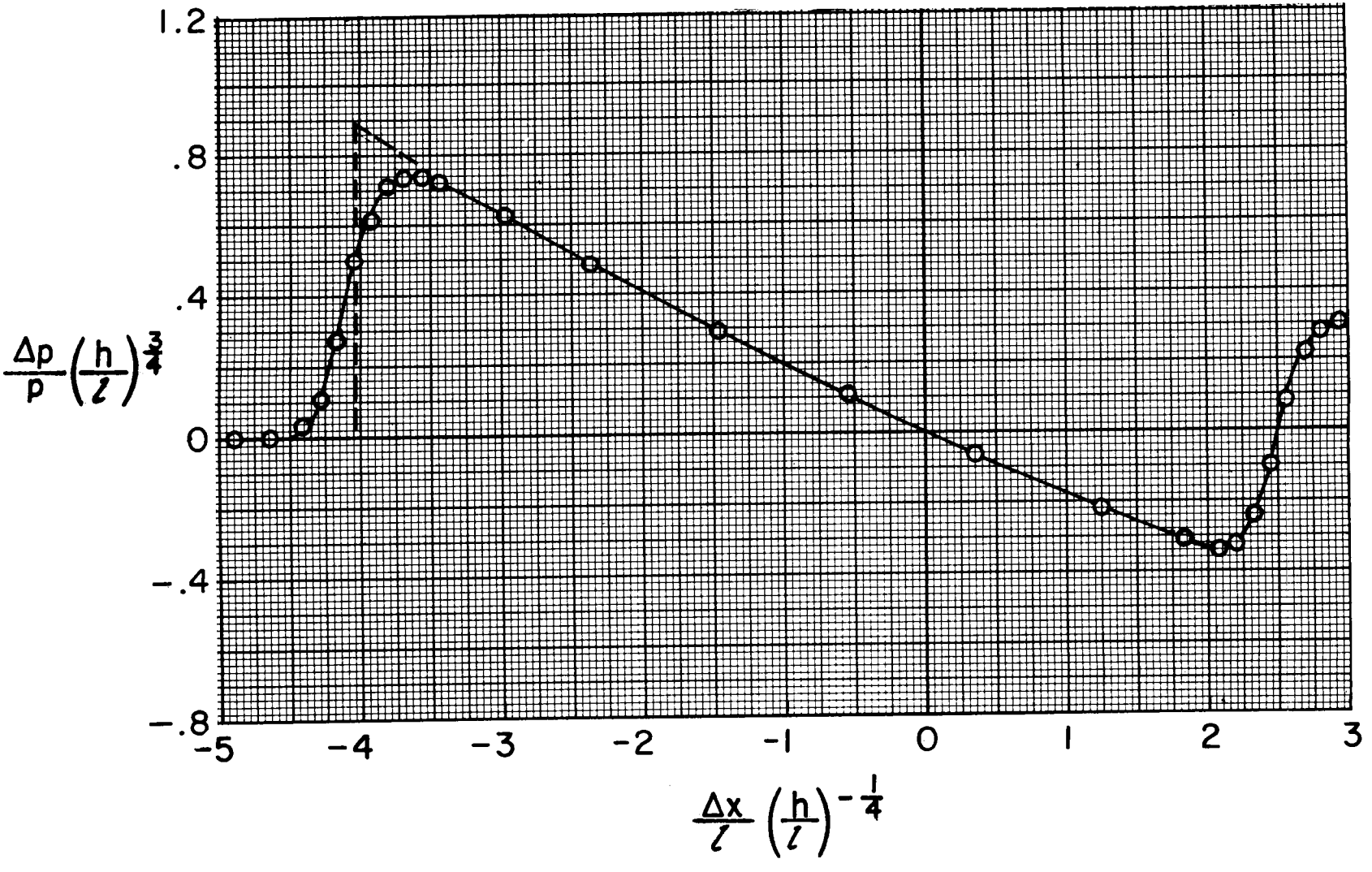

(c) $h/l = 24$.

Figure 11.- Concluded.

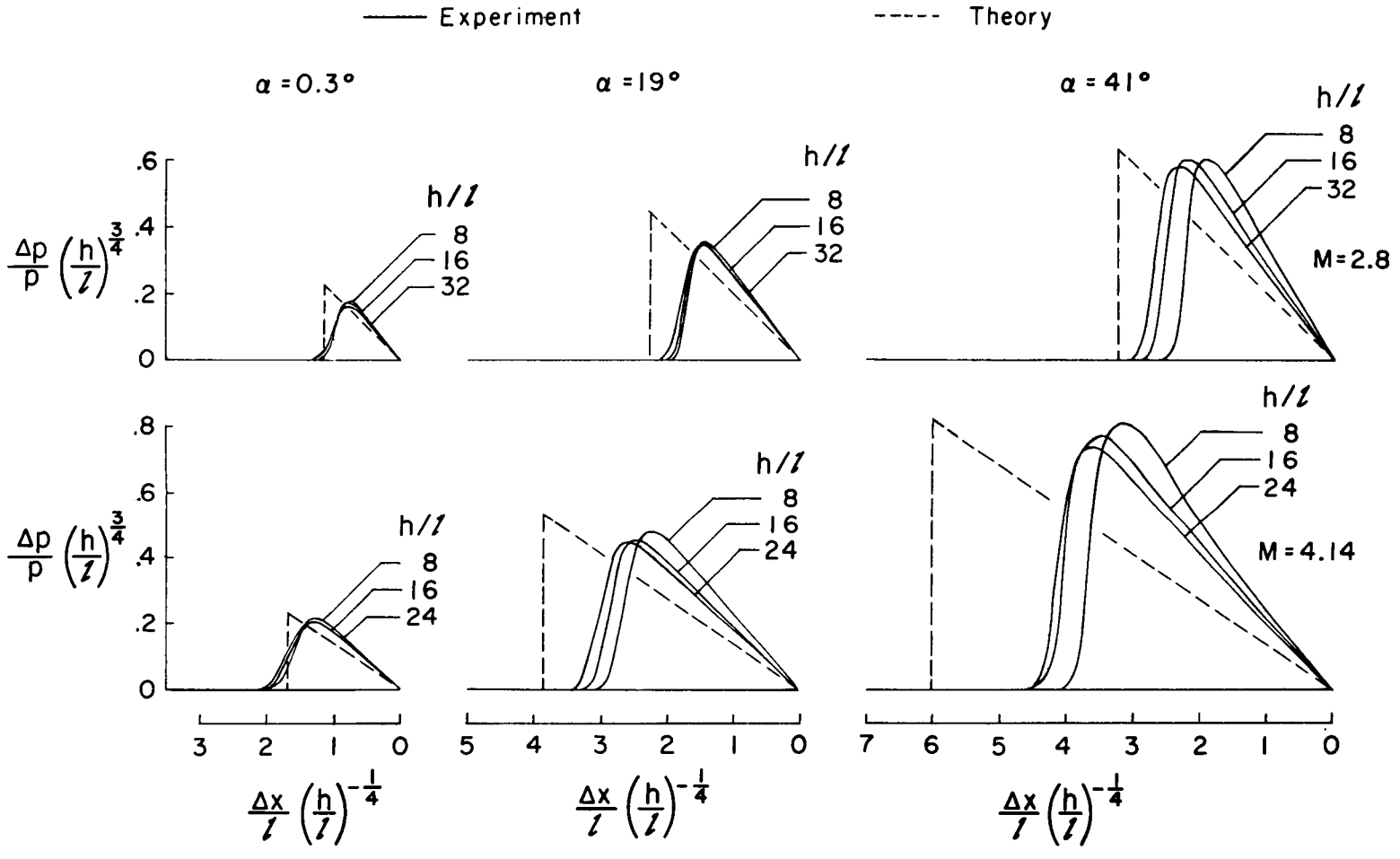

Figure 12.- Correlation of experimental and theoretical pressure signatures.

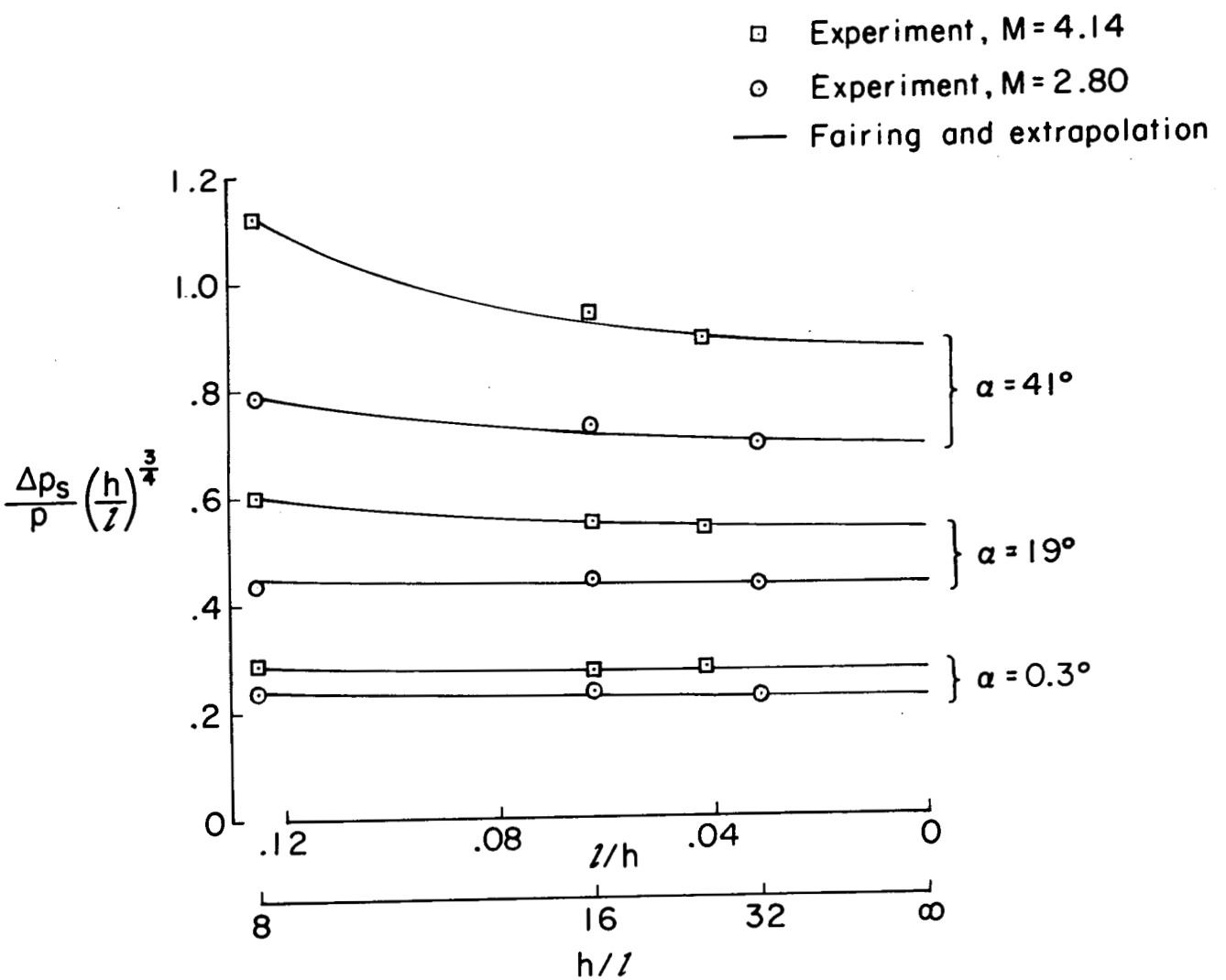

(a) Bow-shock overpressure.

Figure 13.- Extrapolation of adjusted experimental signature parameters.

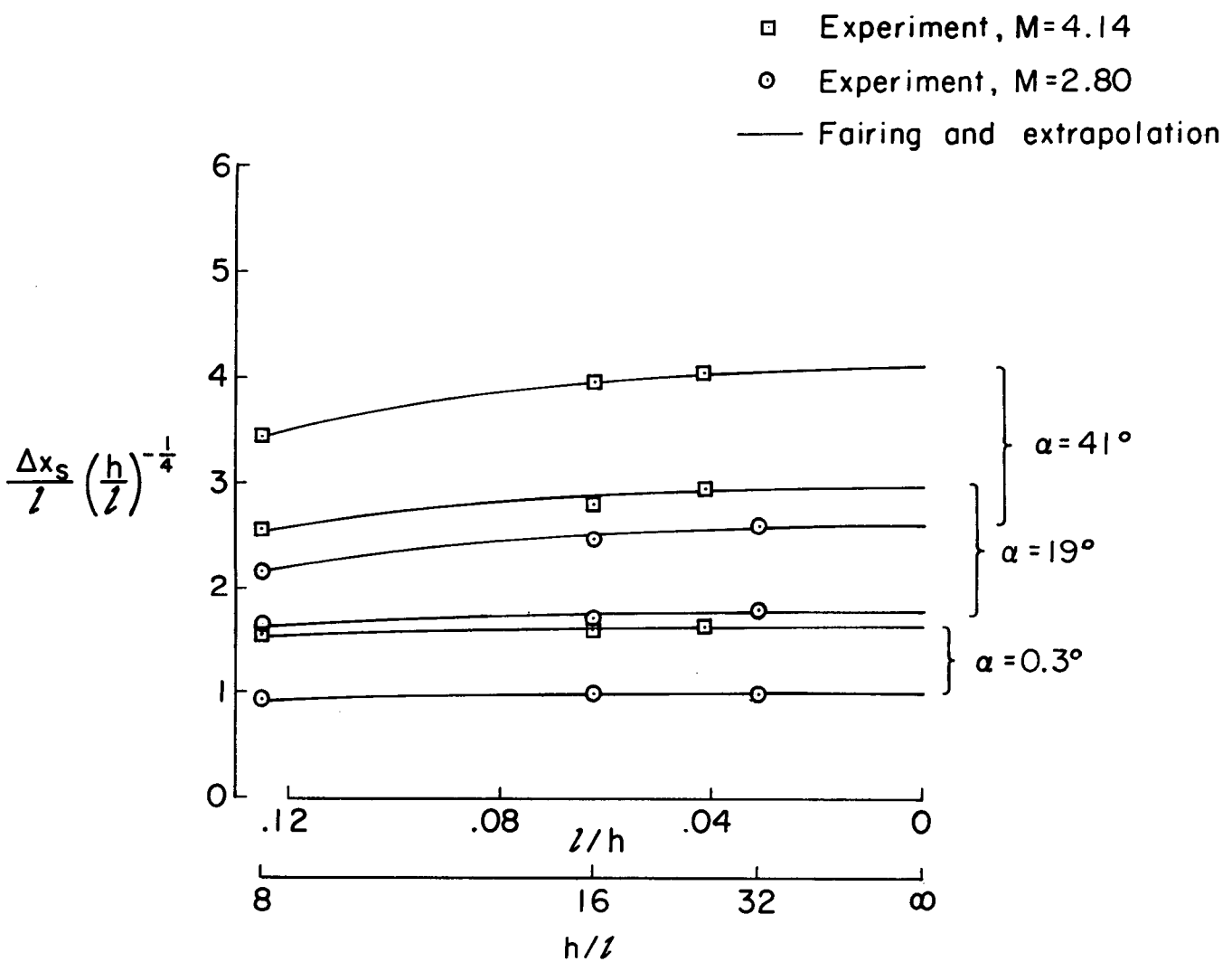

(b) Signature length.

Figure 13.- Continued.

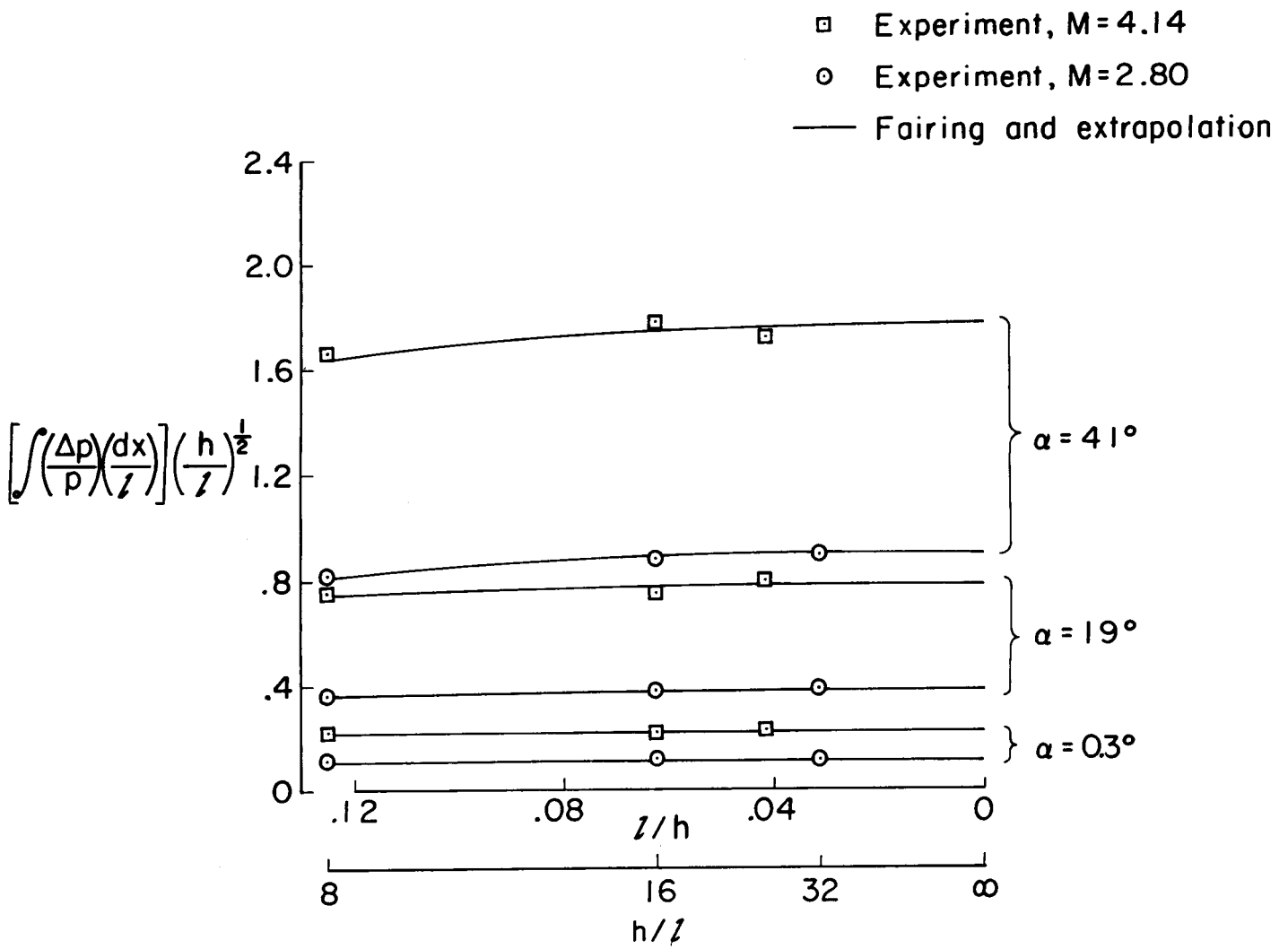

(c) Signature impulse.

Figure 13.- Concluded.

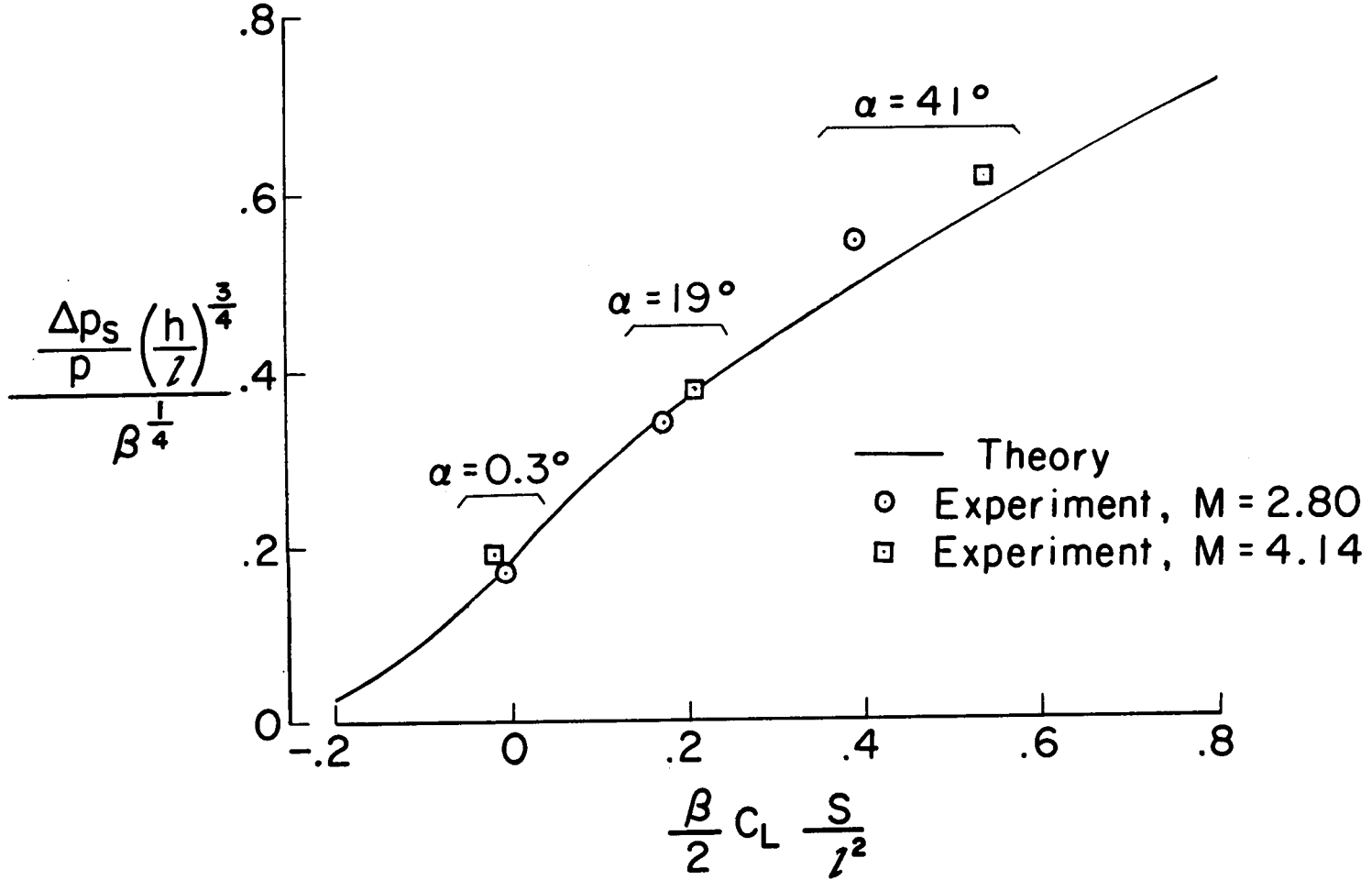

(a) Bow-shock overpressure.

Figure 14.- Correlation of theoretical and extrapolated experimental signature parameters.

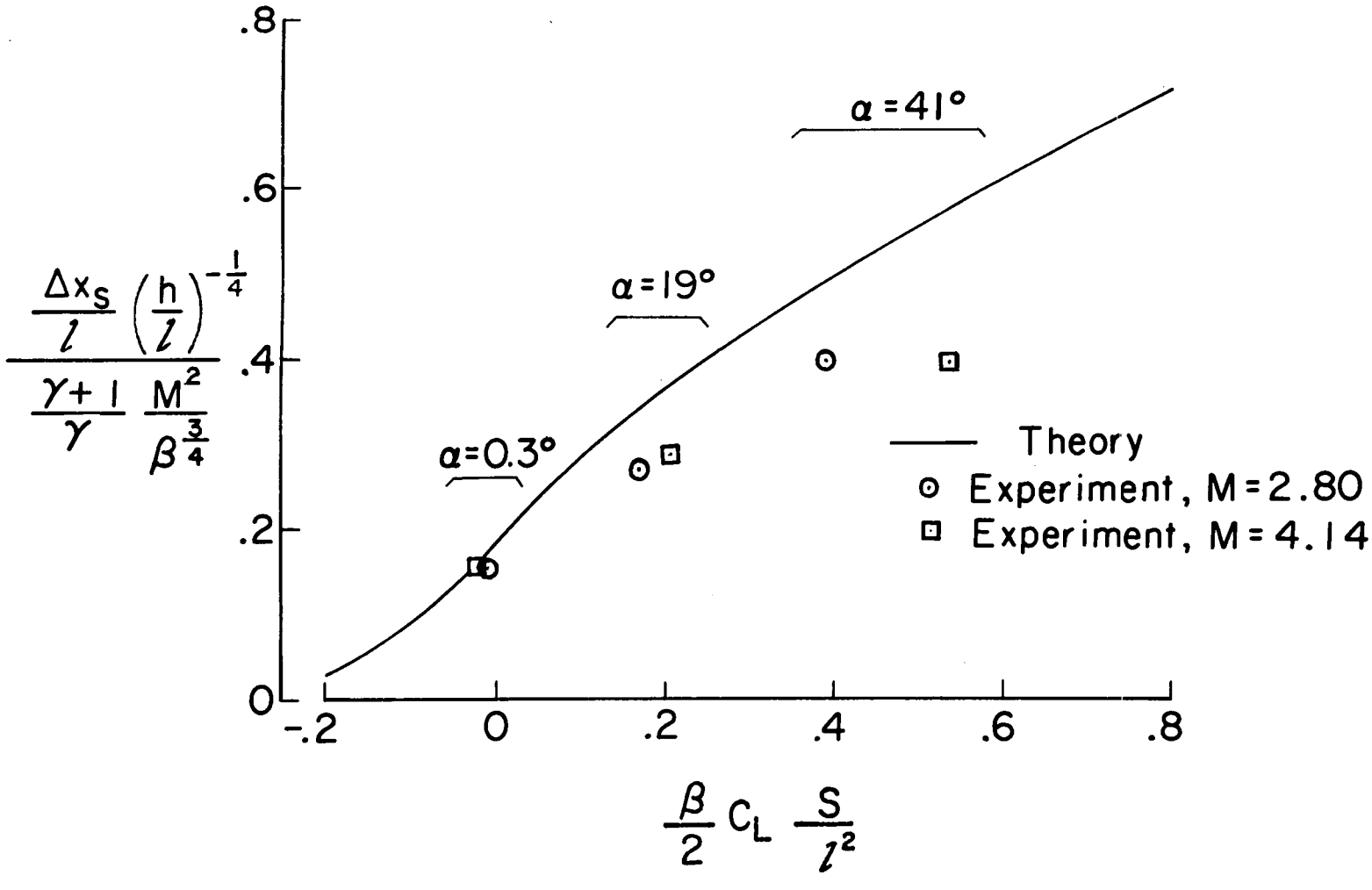

(b) Signature length.

Figure 14.- Continued.

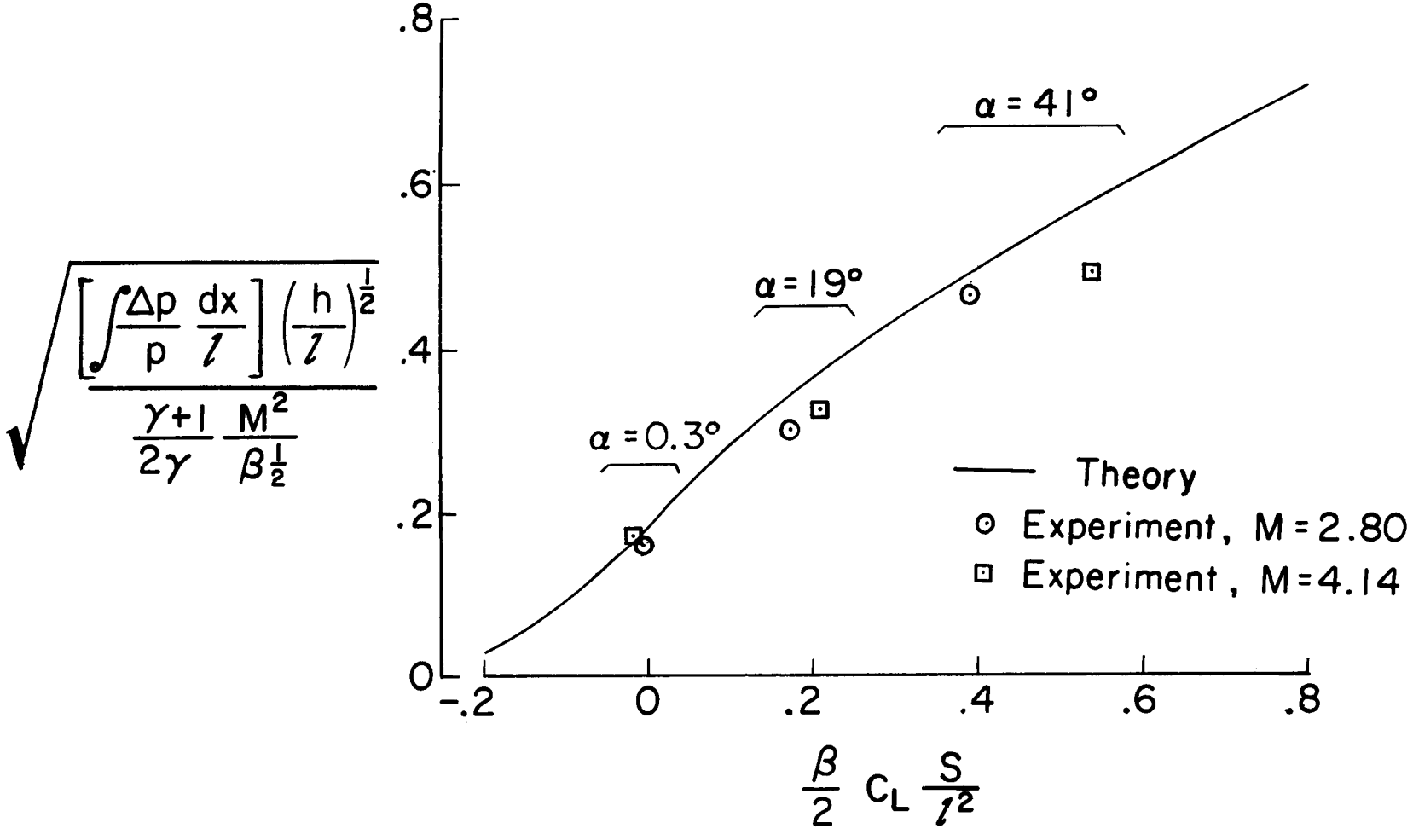

(c) Signature impulse.

Figure 14.- Concluded.

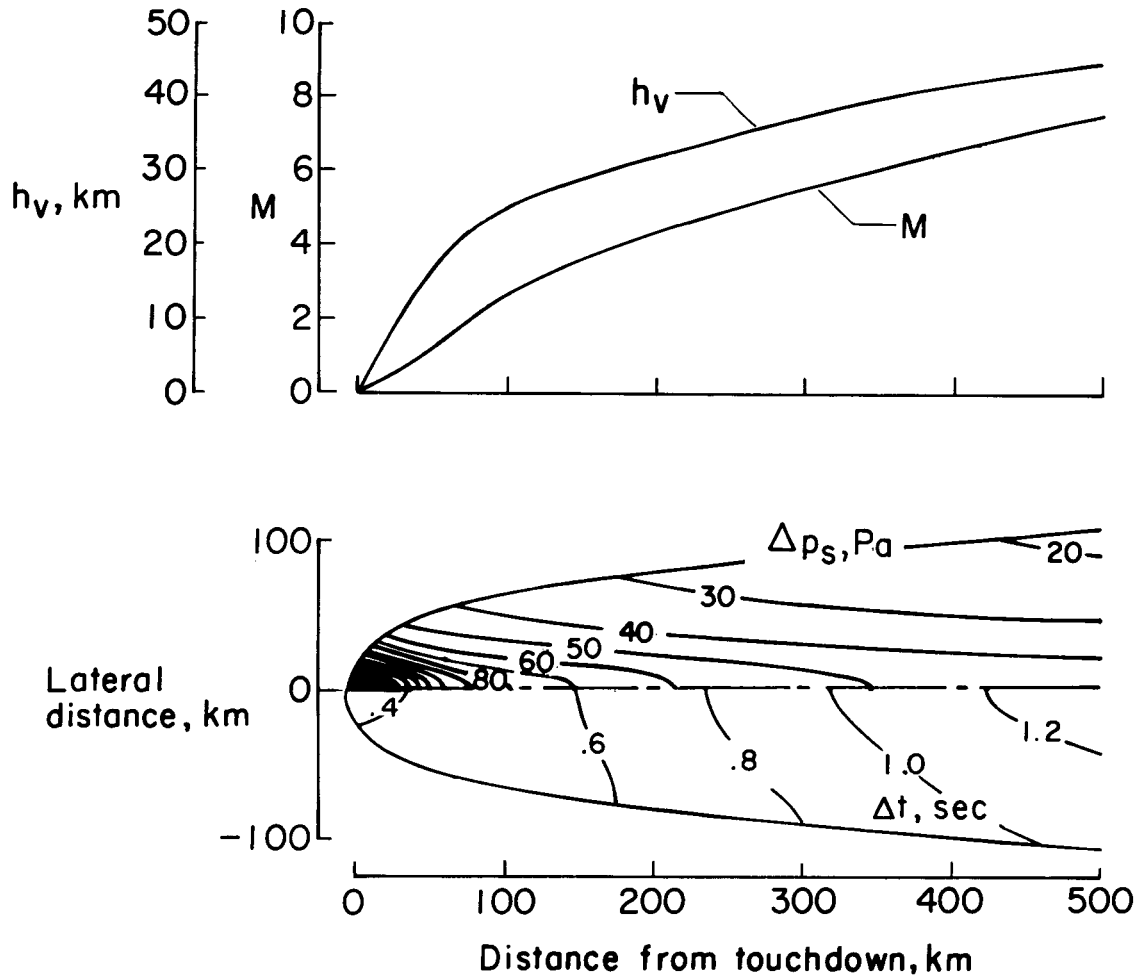

(a) SI Units.

Figure 15.- Estimated sonic-boom footprint for a typical entry flight profile.

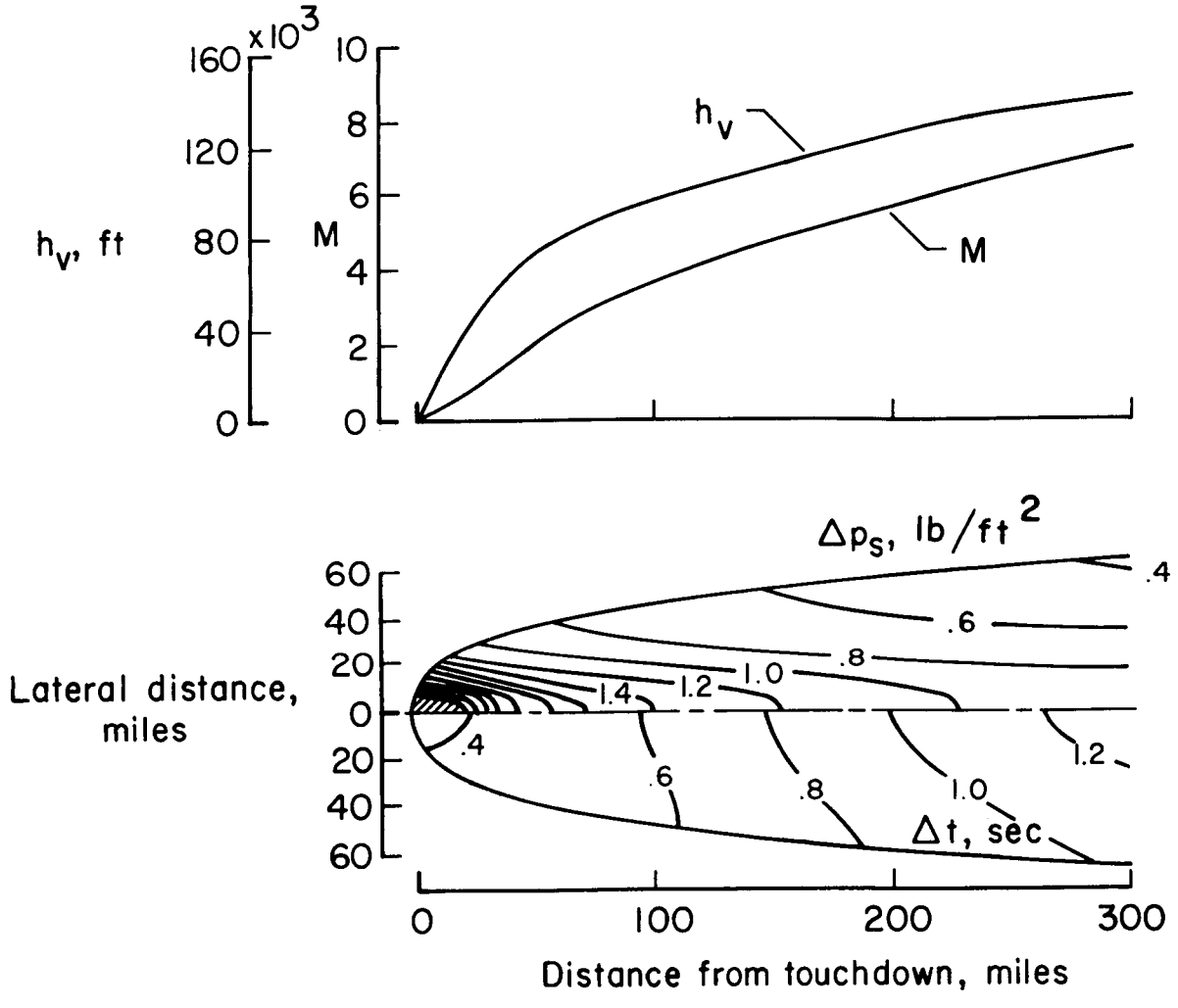

(b) U.S. Customary Units.

Figure 15.- Concluded.

1. Report No.	2. Government Accession No.	3. Recipient's Catalog No.
NASA TP-1186		

4. Title and Subtitle	5. Report Date
A WIND-TUNNEL STUDY OF THE APPLICABILITY OF FAR-FIELD SONIC-BOOM THEORY TO THE SPACE SHUTTLE ORBITER	June 1978
	6. Performing Organization Code

7. Author(s)	8. Performing Organization Report No.
Harry W. Carlson and Robert J. Mack	L-12051
	10. Work Unit No. 743-04-13-04

9. Performing Organization Name and Address	11. Contract or Grant No.
NASA Langley Research Center Hampton, VA 23665	

12. Sponsoring Agency Name and Address	13. Type of Report and Period Covered
National Aeronautics and Space Administration Washington, DC 20546	Technical Paper
	14. Sponsoring Agency Code

15. Supplementary Notes

16. Abstract

A wind-tunnel study of the sonic-boom characteristics of a 0.0004-scale model of the space shuttle orbiter has been conducted. Pressure signatures were measured at Mach numbers of 2.8 and 4.14 and at angles of attack of 0.3°, 19.0°, and 41.0°. To allow for observation of signature development and to provide data for extrapolation to larger distances, measurements were made at distances of from 8 to 32 body lengths. Relatively simple, purely theoretical prediction methods provided reasonably accurate estimates of bow-shock overpressure and signature impulse.

17. Key Words (Suggested by Author(s))	18. Distribution Statement
Sonic boom Space shuttle	Unclassified - Unlimited Subject Category 02

19. Security Classif. (of this report)	20. Security Classif. (of this page)	21. No. of Pages	22. Price*
Unclassified	Unclassified	45	$4.50

* For sale by the National Technical Information Service, Springfield, Virginia 22161

NASA-Langley, 1978